

RESEARCH ARTICLE

Insights into the evolution of metazoan regenerative mechanisms: roles of TGF superfamily members in tissue regeneration of the marine sponge *Chondrosia reniformis*

Marina Pozzolini^{1,*}, Lorenzo Gallus¹, Stefano Ghignone², Sara Ferrando¹, Simona Candiani¹, Matteo Bozzo¹, Marco Bertolino¹, Gabriele Costa¹, Giorgio Bavestrello¹ and Sonia Scarfi¹

ABSTRACT

Tissue repair is an adaptive and widespread metazoan response. It is characterised by different cellular mechanisms and complex signalling networks that involve numerous growth factors and cytokines. In higher animals, transforming growth factor- β (TGF- β) signalling plays a fundamental role in wound healing. In order to evaluate the involvement of TGF superfamily members in lower invertebrate tissue regeneration, sequences for putative TGF ligands and receptors were isolated from the transcriptome of the marine sponge *Chondrosia reniformis*. We identified seven transcripts that coded for TGF superfamily ligands and three for TGF superfamily receptors. Phylogenetically, *C. reniformis* TGF ligands were not grouped into any TGF superfamily clades and thus presumably evolved independently, whereas the TGF receptors clustered in the Type I receptor group. We performed gene expression profiling of these transcripts in sponge regenerating tissue explants. Data showed that three ligands (TGF1, TGF3 and TGF6) were mainly expressed during early regeneration and seemed to be involved in stem cell maintenance, whereas two others (TGF4 and TGF5) were strongly upregulated during late regeneration and thus were considered pro-differentiating factors. The presence of a strong TGF inhibitor, SB431542, blocked the restoration of the exopinacoderm layer in the sponge explants, confirming the functional involvement of the TGF pathway in tissue regeneration in these early evolved animals.

KEY WORDS: TGF- β , TGF- β -receptors, Tissue regeneration, Porifera, Metazoan evolution

INTRODUCTION

Regenerative tissue repair is an adaptive and widespread response in all metazoan taxa; it presents numerous mechanisms and potentialities (Vervoort, 2011). Reconstitution and/or replacement of lost structures and tissues through regeneration is a complex physiological process that involves myriad cell types, cellular mechanisms and molecular effectors (Tanaka and Reddien, 2011). Soluble mediators are released at different regeneration phases, influence wound cells through autocrine and paracrine


mechanisms, and control and coordinate the process (Grotendorst et al., 1988; Matsuoka and Grotendorst, 1989). Knowledge about the evolutionary history of the diverse regeneration mechanisms among animals requires the study of these processes in early evolved metazoans. Marine sponges (Porifera) are considered among the oldest extant metazoans (Müller, 1998) and display an attractive and suitable model for tissue regeneration.

Sponges are widely distributed in marine and freshwater ecosystems (Van Soest et al., 2012). The ecological success of these animals is due to their remarkable morphological plasticity (Gaino and Burlando, 1990) and their high tissue regeneration properties (Nickel and Brümmer, 2003). Sponge regenerative processes have been studied mainly at the morphological level with an *in vitro* system of 3-D cell aggregates called Primmorph (Custodio et al., 1998; Pozzolini et al., 2014; Zhang et al., 2003), small tissue explants (Nickel and Brümmer, 2003) or surgically injured whole organisms (Borisenko et al., 2015). Fine ultrastructural studies conducted on the demosponge *Halisarca dujardini* revealed that wound repair is a complex process that includes multiple combined cellular mechanisms, such as the epithelial-to-mesenchymal transition (EMT) and mesenchymal-to-epithelial transition (MET) (Borisenko et al., 2015). In the Homoscleromorpha class, the main cellular mechanisms involved in exopinacoderm restoration are exopinacocyte spreading and choanocyte transdifferentiation. (Ereskovsky et al., 2015). Kenny et al. (2018) applied a molecular approach to sponge morphogenesis and performed the first differential transcriptome sequencing on the encrusting reef sponge *Halisarca caerulea*.

Among the main soluble molecular effectors involved in wound healing and regenerative processes in higher animals, transforming growth factor- β (TGF- β) plays a fundamental role (O’Kane and Ferguson, 1997). TGF- β is a small, secreted dimeric signalling protein that controls myriad cellular processes, including proper embryonic tissue and organ development (Kaartinen et al., 1995; Sanford et al., 1997), adaptive immune system regulation in adult organisms (Letterio and Roberts, 1998) and fibrogenesis (Pohlers et al., 2009). It is a member of the TGF superfamily. Researchers have identified TGF superfamily members in diverse animals including ctenophores (Pang et al., 2011), flies (Upadhyay et al., 2017), nematodes (Savage-Dunn and Padgett, 2017) and lower vertebrates (Hino et al., 2003). Invertebrate TGF superfamily members share a function similar to that of mammalian counterparts and are all related and diversified from common ancestral genes (Hinck, 2012). Members of the TGF- β signalling pathway are found in Porifera (Suga et al., 1999). In these animals, TGF- β , together with Wnt, influences axial polarity during embryonic and larval development (Adamska et al., 2007).

¹Department of Earth, Environment and Life Sciences (DISTAV), University of Genova, Via Pastore 3, 16132 Genova, Italy. ²Institute for Sustainable Plant Protection-Turin Unit (CNR), Viale Mattioli 25, 10125 Torino, Italy.

*Author for correspondence (marina.pozzolini@unige.it)

 M.P., 0000-0001-6867-3816; L.G., 0000-0003-4496-3602; S.G., 0000-0002-2033-2286

The present study aimed to investigate tissue regeneration in sponges at the molecular level, and in particular to establish the involvement of TGF- β signalling in this process. For this purpose, tissue regeneration was analysed in the marine sponge *Chondrosia reniformis* Nardo 1947, a member of the Demospongiae. *Chondrosia reniformis* lacks the silica spicules that strengthen the body in most other species of the same class. Its body is mainly composed of tightly packed collagenous fibres; *C. reniformis*-derived collagen is the most widely studied among all sponges (Imhoff and Garrone, 1983; Swatschek et al., 2002), and its use has been widely described for biotechnological applications (Kreuter et al., 2000; Nicklas et al., 2009; Pozzolini et al., 2018). This species exhibits marked regenerative properties. Indeed, *C. reniformis* tissue explants can be cultured *in vitro* (Nickel and Brümmer, 2003) or in aquaria (Pozzolini et al., 2012) to generate a large number of clones derived from the same specimen. Further studies identified various transcripts involved in fibrogenesis (Pozzolini et al., 2012, 2015, 2016a) as well as in siliceous sediment management (Pozzolini et al., 2016b, 2017).

In the present work, TGF ligand and TGF receptor (TGF β) superfamily members were identified in the *C. reniformis* transcriptome, and their gene expression profile, coupled with ultrastructural observations, was analysed in *C. reniformis* regenerating tissue explants (RTEs). Finally, to confirm their functional implication in sponge regeneration, the same analyses were performed in the presence of a specific TGF inhibitor.

MATERIALS AND METHODS

TGF ligand and receptor superfamily member identification

TGF ligand and receptor superfamily members were identified from the previously sequenced and assembled *C. reniformis* transcriptome (Pozzolini et al., 2016a,b). For TGF ligands, the putative transcript from *Amphimedon queenslandica* and bilaterian gene orthologues were used as a query in tblastn searches of the *C. reniformis* transcriptome. Candidate TGF β transcripts were directly identified through sequence homology searches with the BLAST suite (NCBI; <http://blast.ncbi.nlm.nih.gov/Blast.cgi>).

Phylogenetic analysis

Phylogenetic placement of *C. reniformis* TGF ligand and receptor superfamily members was obtained using a previously published Bayesian analysis of TGF- β ligands and receptors of the ctenophore *Mnemiopsis leidyi* (Pang et al., 2011), along with other homologous ligands and receptors available from sponge transcriptomes. For this purpose, the transcriptomes from *Aphrocallistes vastus*, *Chondrilla nucula*, *Corticium candelabrum*, *Sarcotragus fasciculatus*, *Petrosia (Petrosia) ficiformis*, *Pseudospongosorites suberitoides* (Riesgo et al., 2014) and *Halisarca caerulea* (Kenny et al., 2018) were analysed with TRANSDCODER V.5.2.0 (<https://github.com/TransDecoder/TransDecoder>) to extract likely coding regions from transcripts and to identify coding sequences with homology to known protein domains via Pfam searches. Pfam annotations were searched for the terms 'TGF β ' (ligand) and 'TGF β GS' (receptor), and only high-scoring complete or partial 5' predicted candidate peptides for both classes were selected (see Table S3).

Putative *C. reniformis* TGF ligand and receptor members and other sponge candidate ligand and receptor homologues were added with MAFFT V.7 (<https://mafft.cbrc.jp/alignment/server/add.html>) to the alignments from figs 2 and 4 in Pang et al. (2011). For TGF- β ligands, only the mature 3'-terminal TGF- β -peptide domain was used in phylogenetic analyses. Alignment refinements were made with JALVIEW V.2.10.5 (Waterhouse et al., 2009). Bayesian

inference was performed for ligands and receptors with MRBAYES V.3.2 (Rohnquist and Huelsenbeck, 2003), using the amino acid 'mixed' model, gamma substitution rates and six ngammacat (the number of discrete categories used to approximate the gamma distribution), with four independent runs of five million generations and trees sampled every 100 generations. Gaps were treated as missing data. Consensus tree visualisation and editing were performed with FIGTREE V.1.4.2 (<http://tree.bio.ed.ac.uk/software/figtree/>).

Sponge collection, transport and aquarium storage

Chondrosia reniformis specimens were collected around the Portofino Promontory (Liguria, Italy) at 10–20 m depth and quickly transferred to the laboratory in a cooler. During transport, the temperature was maintained at 14–15°C. Sponges were stored in a 250 litre aquarium, equipped with an aeration system, which contained natural seawater collected in the same area of the Portofino Promontory at 14°C with 37‰ salinity.

Experimental regeneration conditions

Chondrosia reniformis specimens were transferred to plastic containers that contained filtered natural seawater (FNSW). The sponges were cut into cylindrical fragments of 9 mm diameter using a sterilised brass borer, quickly transferred to an aquarium (in 12-well plates) and allowed to regenerate for 3, 9, 24, 48, 72 or 144 h (Fig. S1).

Histological analyses

Chondrosia reniformis intact samples and RTEs were recovered from the aquarium, washed with FNSW and fixed in 4% paraformaldehyde (Carlo Erba Reagents, Milan, Italy) in 0.1 mol l⁻¹ phosphate buffered saline (PBS; pH 7.4) overnight at 4°C. Specimens were then embedded in Paraplast (McCormick, IL, USA) at 56°C and sectioned at 6 μ m. Slides for light microscopy were stained with Haematoxylin and Eosin (H&E), Picro Sirius Red (PSR) for collagen (Junqueira et al., 1979) and Masson's Trichrome (MT) to highlight the internal *C. reniformis* anatomy. The PSR method differentially stains various collagen fibres. Specifically, in bright-field microscopy, collagen appears red, whereas under cross-polarised light microscopy, birefringence leads the larger collagen fibres (type I collagen) to appear bright yellow or orange, while the thinner fibres, including reticular fibres (type III collagen), appear green (Junqueira et al., 1979). All stained sections were visualised with a Leica DMRB light and epifluorescence microscope (Leica microsystems, Milan, Italy) equipped with cross polarisers and Nomarski differential interference contrast (DIC) filters; the objective was a 40 \times Leica air with a 0.65 numerical aperture. The images were acquired with a Leica CCD camera (model DFC420C).

Transmission electron microscopy (TEM) negative staining

For TEM observation, *C. reniformis* samples were fixed in 2% paraformaldehyde and 2.5% glutaraldehyde in 0.1 mol l⁻¹ PBS (pH 7.4) for 4 h at 4°C and then washed three times in PBS. The samples were impregnated with 2.3 mol l⁻¹ sucrose (in PBS), frozen in liquid nitrogen and cryosectioned with an ultramicrotome (Reichert-Jung Ultracut E with an FC4E attachment). The ultra-thin cryosections were collected on carbon-coated copper grids, treated with 2% paraformaldehyde in 0.1 mol l⁻¹ PBS (pH 7.4) for 20 min at room temperature and washed in PBS. The grids were partially dried, washed by touching them three times on the surface of a drop of distilled water, then contrasted with 2% uranyl acetate in 0.15 mol l⁻¹ oxalic acid for 5 min and then 5 min in a 9:1 mixture of

2% uranyl acetate and 25 cP methylcellulose. Samples were observed with a Philips CM10 TEM equipped with a Megaview 3 camera and iTEM Olympus SIS digital imaging software.

Environmental scanning electron microscopy (ESEM)

For ESEM, RTEs were washed with FNSW and fixed with a mixture of 2% paraformaldehyde and 2.5% glutaraldehyde in PBS (pH 7.4) for 30 min and dehydrated by passing through a series of increasing ethanol concentrations (up to 100%). The samples were further dehydrated to the critical point, graphite covered and observed with an ESEM Vega3–Tescan, type LMU (Tescan, Brno s.r.o., Czech Republic) equipped with an EDS-Apollo_x micro-analyser system and EDS Texture and Elemental Analytical Microscopy software (TEAM).

Choanocyte identification by India ink staining

Choanocyte cell bodies in live *C. reniformis* specimens were marked with a commercial ink that consisted of a carbon black solution (Winsor & Newton, Drawing Ink Bottle), according to Ereskovsky et al. (2015). Choanocytes incorporate the carbon black and keep it internally (specifically in phagosomes) until, having exhausted their approximately 8-h life cycle, they disperse the ink through exhaling channels or maintain it in the choanoderm/mesohyl matrix if engaged in transdifferentiation. Intact sponges were incubated in FNSW that contained 2% India ink for 12 h before the experiments. We observed that a 12-h incubation allowed the choanocytes enough time for dye internalisation. The marked specimens were washed in fresh seawater several times. Samples kept as controls did not show any signs of suffering. The marked specimens were finally used for tissue explant preparation and incubated according to the experimental protocol (0, 3, 9, 24, 48 or 72 h); the samples were observed after paraffin embedding and sectioning, without further staining, by DIC microscopy.

Archeocyte identification by immunostaining

Previous studies indicated that the Musashi gene (*Msi-1*) is specifically expressed in sponge stem cells (archoocytes; Okamoto et al., 2012) and that it can be considered an archeocyte-specific molecular marker. In order to identify archeocytes in *C. reniformis* RTEs, a candidate *C. reniformis Msi-1* transcript (an MH687926) was identified (Pozzolini et al., 2016a,b). The predicted *C. reniformis Msi-1* protein was aligned with human Msi-1 (UniProtKB, O43347) using the LALIGN server to determine whether the antisera could recognise Msi-1 in sponge tissues; the identity level was 29.5%. Indirect immunohistochemical reactions were performed using the polyclonal rabbit anti-Msi-1 antiserum (E-AB-17518-60; Invitrogen). This antiserum was raised against amino acids from the human Msi-1 N-terminus. The secondary antibody was Alexa 488-conjugated chicken anti-rabbit antiserum (1:800 in PBS; Molecular Probes, Invitrogen). As a negative control, the primary antiserum was omitted (Saper, 2009; Saper and Sawchenko, 2003).

Quantitative real-time polymerase chain reaction (qPCR) gene expression analysis

Total RNA was extracted from *C. reniformis* RTEs using Isol-RNA Lysil (5'-Prime, Eppendorf srl, Milan, Italy), according to the manufacturer's instructions. Subsequently, the poly-A fraction was isolated using the FastTrack[®] MAG messenger RNA (mRNA) isolation kit (Life Technologies, Milan, Italy). Complementary DNA (cDNA) was obtained by reverse transcription with the iScript cDNA Synthesis kit (Bio-Rad Laboratories, Milan, Italy),

according to the manufacturer's protocol, using 200 ng of purified mRNA. *GAPDH* (accession number KM217385) was used as the reference gene for sample normalisation. Reactions, in a 20 µl volume, contained 1× iQ SYBR Green master mix (Bio-Rad Laboratories), 0.2 µmol l⁻¹ of each primer and 0.8 µl cDNA. All samples were analysed in triplicate. Thermal cycling conditions were initial denaturation at 95°C for 3 min followed by 45 cycles with denaturation at 95°C for 15 s and annealing and elongation at 60°C for 60 s. Fluorescence was measured at the end of each elongation step. The next step was a slow heating (1°C s⁻¹) of the amplified product from 55 to 92°C to generate a melting curve. All primers were designed using Beacon Designer 7.0 (Premier Biosoft International, Palo Alto, CA, USA) using default parameters for SYBR Green reactions (GC %: 45–55%, *T_m*: 58–62°C, product length: 80–100 bp). They were then synthesised by TibMolBiol (Genova, Italy). The primer sequences for *GAPDH*, fibrillar collagen and non-fibrillar collagen were reported in Pozzolini et al. (2016a,b), while primers for proline-4 hydroxylase (*P4H*) and *Bcl-2* were reported in Pozzolini et al. (2017). The *TGF1*, *TGF2*, *TGF3*, *TGF4*, *TGF5*, *TGF6*, *TGFR1*, *TGFR2*, *Piwi* and *Msi-1* primer sequences are presented in Table S1. Data analyses were obtained using the DNA Engine Opticon[®] 3 Real-Time Detection System Software (V3.03). Relative gene expression profiles in regenerating tissue were compared with a steady-state calibrator sample (control, C) using the *C_t* method (Aarskog and Vedeler, 2000) with Gene Expression Analysis software for iCycler iQ Real Time Detection System (Bio-Rad Laboratories) (Vandesompele et al., 2002).

The relative mRNA level of the various TGF ligands and receptors in *C. reniformis* steady-state tissue was evaluated by comparing the *C_t* values obtained from qPCR for each transcript and expressed as fold increase relative to the gene that had the highest *C_t* value (*TGF4*), and therefore the lowest expression level. Thus, the value of the fold increase for each transcript with respect to *TGF4* mRNA was calculated as:

sample fold increase = $2^{(C_{t,TGF4} - C_{t,s})}$, where *C_{t,TGF4}* is the *C_t* value for *TGF4* and *C_{t,s}* is the *C_t* value for all other transcripts.

Tropocollagen assay

Newly synthesized tropocollagen in *C. reniformis* RTEs was assayed with a colorimetric method using the Sircol Assay (Biocolor Ltd, Carrickfergus, County Antrim, UK), as previously described (Pozzolini et al., 2017). The collagen content was then normalised to the weight of the wet tissue explants.

In situ hybridisation

In order to evaluate *TGF6* mRNA tissue localisation, *C. reniformis* RTEs were analysed using *in situ* hybridisation, as described by Candiani et al. (2015). *Chondrosia reniformis* RTEs were recovered at 0, 24, 48 or 72 h post-excision and washed with FNSW. After fixation overnight at 4°C in 4% paraformaldehyde in PBS (pH 7.4), the samples were rinsed with PBS, immersed in 20% sucrose at 4°C and then embedded in 20% sucrose/Killik (inclusion medium for cryostatic cutting, Bio-Optica, Italy) in a 1:1 ratio for 2 h at room temperature, and finally in 100% Killik in cryogenic moulds and frozen in liquid nitrogen. Samples were sectioned at 10 µm with a Leica CM1900 cryostat.

The air-dried slides were washed and treated for 20 min with RIPA buffer (150 mmol l⁻¹ NaCl, 5 mmol l⁻¹ EDTA, 50 mmol l⁻¹ Tris-Cl, 1% IGEPAL CA-630, 0.5% sodium deoxycholate and 0.1% SDS). Then, sections were post-fixed for 10 min in 4% paraformaldehyde in PBS, washed in PBS and then treated with

0.25% acetic anhydride and 0.1 mmol l⁻¹ triethanolamine for 15 min, washed in PBS and pre-hybridised with hybridisation buffer [50% formamide, 5× saline-sodium citrate (SSC), 0.5 mg ml⁻¹ Torula yeast RNA, 50 µg ml⁻¹ heparin and 0.1% Tween-20] at 60°C for 5 h. The sections were subsequently incubated with the sense or antisense riboprobe in hybridisation buffer overnight at 60°C. The slides were then washed for 1 h in post-hybridisation buffer (50% formamide, 2X SSC and 0.1% Tween-20 0.1%), 20 min in MABT (1 mol l⁻¹ maleic acid pH 7.5, 5 mol l⁻¹ NaCl and 0.1% Tween-20) and blocked with blocking solution (10% fetal bovine serum in MABT) for 5 h. The sections were next incubated with an alkaline-phosphatase-conjugated anti-digoxigenin antibody (1:500 in blocking solution) overnight at 4°C. The sections were rinsed in MABT and washed with AP buffer (100 mmol l⁻¹ Tris pH 9.6, 50 mmol l⁻¹ MgCl₂, 100 mmol l⁻¹ NaCl and 0.1% Tween-20) for 45 min and stained with NBT/BCIP solution (187 µg ml⁻¹ NBT and 175 µg ml⁻¹ BCIP in AP buffer) for variable times. Staining was terminated by washing in PBST (0.1% Tween-20 in PBS). The slides were post-fixed with 4% paraformaldehyde for 10 min, washed with PBS and finally mounted in PBS with 70% glycerol and 0.1% sodium azide.

Sense and antisense digoxigenin-RNA probes were prepared using the DIG-RNA Labeling Kit (Roche Applied Science, Monza, Italy) according to the manufacturer's instructions. We amplified a PCR DNA fragment of 662 bp from the isotig12606 (nucleotides 41–661, MH687922 in GenBank) with RNA polymerase promoter S6/T7 sequences at each end, providing a single template for the *in vitro* synthesis of either sense or antisense cRNA probes.

Effect of TGF inhibitor

In order to evaluate the functional involvement of TGF ligands on sponge tissue regeneration, *C. reniformis* RTEs obtained as previously described were placed in a 6-well plate in FNSW in the presence of 0.1 mmol l⁻¹ SB431542, a potent inhibitor of TGF-β signalling that blocks type I receptor activity (Inman et al., 2002), and transferred to a 14°C incubator for 24, 72 or 144 h.

Statistical analysis

Experiments were performed three times in triplicate. The results were analysed by paired *t*-test versus the respective controls or alternatively by one-way ANOVA followed by a paired Tukey test. *P*-values <0.05 were considered significant.

RESULTS

Putative TGF ligand and receptor identification

Examination of the *C. reniformis* assembled transcriptome revealed seven putative TGF ligands and three TGF receptors (Table S2). Isotig04814 and isotig04815 diverged from each other by only 90 bp at the 5'-end; thus, we reasonably considered them as alternative splicing products of the same gene. In the text and Table S2, they are referred to as *TGF1*. Similarly, isotig01962 and isotig01963 diverged from each other by only 45 bp at the 3'-end and again were considered to derive from the same gene (*TGFR1*). *TGF1*, *TGF2* and *TGF3* sequences were complete, whereas *TGF4*, *TGF5*, *TGF6*, *TGFR1* and *TGFR2* lacked a complete 5'-end. The sequences were deposited in GenBank (accession numbers in Table S2). Homology searches using SMART (Letunic et al., 2008) on the putative amino acid sequences of the six *C. reniformis* TGF ligands predicted the presence of a signal peptide in the complete *TGF1*, *TGF2* and *TGF3* sequences (Fig. S3A). The TGF-β pro-peptide was identified only in *TGF3*, whereas in *TGF1* and *TGF2* the pro-peptide was missing or highly divergent and not detected by

sequence homology search. TGF-β peptides were found in all six TGF ligands. A multiple sequence alignment among TGF-β peptides derived from the six *C. reniformis* TGF ligands and TGF-β peptide from human TGF-β (Fig. S3B) revealed the presence of the typical seven conserved cysteines in all sponge TGF ligands except for *TGF1* and *TGF2*, where the fourth residue was replaced by a lysine or a serine, respectively. The TGF-β peptide cleavage site RXXR is clearly present in all ligands except for *TGF3*, where the sequence is IVKR.

Overall, performing a binary alignment by lalign program (https://embnet.vital-it.ch/software/LALIGN_form.html), *C. reniformis* TGF ligands exhibited an average of 21.5% homology with human TGF-β (NP_000651), while TGFRs displayed an average 38.55% homology with human TGF-β receptor (NP_001124388).

The relative content of the TGF ligands and receptors in *C. reniformis* steady-state tissue was determined by qPCR (Fig. 1). *TGF1* was the most abundant, 54-fold higher than *TGF4*, the least abundant TGF ligand. *TGF2*, *TGF6* and *TGF3* were 33-, 22- and 18-fold higher, respectively, than *TGF4*. *TGF5* was only 5.2-fold higher than *TGF4*. Regarding TGF-r transcripts, in whole, steady-state sponge tissue, *TGFR1* mRNA was 4-fold higher than *TGFR2*.

Phylogenetic tree

Phylogenetic analysis of TGF-β peptide domains from *M. leidy* depicted in fig. 2 from Pang et al. (2011) showed a rather undefined placement of the only homologous ligand from the poriferan *A. queenslandica* (Aqu) used in the analysis; it did not clearly group into the BMP-like or TGF-β-like clusters. Here, addition of several putative homologues from other poriferan species (Table S3) to the Bayesian analysis was still unable to provide a clear classification of TGF superfamily members (Fig. 1B, tree in collapsed form; Fig. S3A, extended form). Very few sequences (*TGF1* from *C. reniformis*, Hca_comp166946_c0_seq4_p1 from *H. cerulea* and Cnu_12673_p1 from *C. nucula*) clustered with the Aqu sequence, present in the original analysis, with a notably low posterior probability value of 0.79; the placement was unclear. Another candidate ligand from *C. reniformis* (*TGF5*) clustered with *M. leidy* *Tgf2*, which was more basal with respect to members that clustered within BMP-like or TGF-β-like groups. Overall, the tree topology in this study suggests that the division of the TGF superfamily into the TGF-β and BMP clades (as reported by Pang et al., 2011) took place after or independently of Porifera divergence because the sponge transcripts do not fit into any of the groupings. Moreover, we speculate that in Porifera, the various paralogues may have arisen from an ancestral gene, and therefore there are different functions in the same species as we demonstrate in this work. The only exceptions are *C. candelabrum* (Cca) sequences, where one of the transcripts clustered in TGF-β clade, but this phenomenon may be explained because *C. candelabrum* belongs to the Homoscleromorpha, considered the most evolved class of Porifera (Wörheide et al., 2012).

The four *A. queenslandica* receptors included in the Bayesian analysis from Pang et al. (2011) grouped two-by-two into two different clades: Aqu_1.227949 and Aqu_1.227950 into Type I receptors and Aqu_1.224888 and Aqu_1.224889 into Type II receptors. Here, all newly identified putative sponge TGFRs clustered into the Type I group (Fig. 1C, tree in collapsed form; Fig. S3B, tree in extended form). In particular, *C. reniformis* *TGFR1* formed a well-supported cluster with Aqu_1.227950 (posterior probability of 1), along with homologues from *P. suberitoides*, *A. vastus* and *C. nucula*, while *TGFR2*, along with homologues from *H. caerulea*, *C. nucula* and *P. ficiformis*, formed a cluster with Aqu_1.227949 supported by a posterior probability value of 0.99.

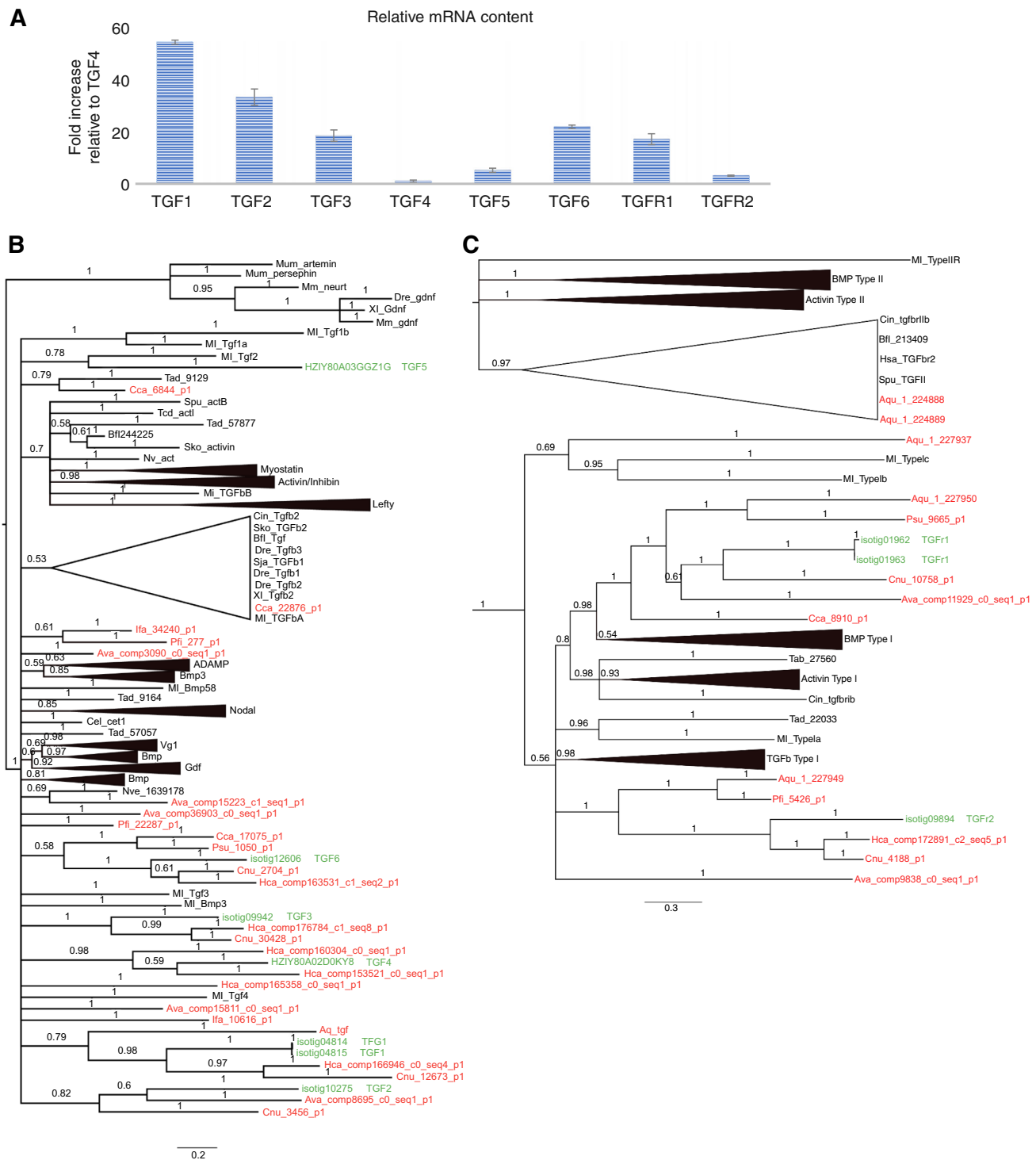


Fig. 1. Relative transforming growth factor (TGF) ligand and receptor mRNA levels in intact sponges and phylogenetic trees. (A) Relative TGF ligand and receptor mRNA levels obtained by qPCR. (B,C) Bayesian inference strict consensus tree for TGF ligands (B) and TGF receptors (C). The phylogenetic trees are derived from the TGF- β peptide domain and receptor (C) alignment used by Pang et al. (2011), and include representative taxa from deuterostomes, protostomes and non-bilaterian organisms (for a full list of taxa, see table S1 in Pang et al., 2011 and Table S2 in the present study). The major clades are collapsed and annotated; the fully expanded version of the trees is provided in Fig. S3. Sponge ligands and receptors are in red, while *Chondrosia reniformis* ligands and receptors identified in this work are in green. Branch support values are given in Bayesian posterior probabilities. The trees are rooted at the midpoint. The bar indicates the number of amino acid substitutions per site.

General *C. reniformis* anatomy and cytology

Chondrosia reniformis is a hard, kidney-shaped sponge without an inorganic skeleton (Fig. S2A). It is formed by an external region called the exopinacodem (Fig. S2B,E,H), which is composed of a

thin layer of flat, small cells termed exopinacocytes or basopinacocytes embedded in a dense mass of collagen fibres, and an internal region (choanoderm) containing the choanocyte chambers (CCs; Fig. S2C,F,G). The choanoderm is formed by a layer of flagellate

cells, the choanocytes, involved in water pumping, and by flat endopinacocytes (Fig. S2G). There are various cell types immersed in the mesohyl between these regions: pluripotent archeocytes (Fig. S2C), collagen-producing lophocytes and spherulous cells (Fig. S2D).

Morphological description of *C. reniformis* exopinacoderm regeneration

During sponge exopinacoderm restoration, there was an initial body contraction 3 h after excision, followed by slow and progressive tissue swelling to a round shape by 144 h (Fig. 2A). According to ultrastructural SEM analysis of the regenerating surface and histological analysis, it is possible to divide the *C. reniformis* exopinacoderm restoration process into three main phases.

Phase I, early stage (0–24 h)

Immediately after excision, the cut surface exhibited dense collagen aggregates with small spherules and bacteria (Fig. 2B). Three hours after excision, thin transverse sections revealed a

jagged and irregular regenerating edge with slime and cellular debris (Fig. 2D). After 9 h, the regenerating border became more compact and homogeneous (Fig. 2F). India ink staining indicated no choanocyte migration to the wound area during this early stage; these cells were located only around the CCs (Fig. 3C,E). After 24 h, SEM analysis showed the presence of various spherules and cells debris at the cut surface that was still composed mainly of collagen aggregates (Fig. 2C). Msi-1 archeocyte immunostaining indicated that immediately after the cut, totipotent archeocytes localised close to the CCs (Fig. 4A) and were absent in the wound area (Fig. 4B).

Phase II, archeocyte migration/differentiation (24–48 h)

During this stage, many Msi-1-positive cells were identified at the regenerating edge (Fig. 4D), an observation that indicates their migration to the wound area from the internal region, where they seemed at this stage less abundant than during phase I (Fig. 4C). After 48 h, the wound surface showed a reduced level of spherules

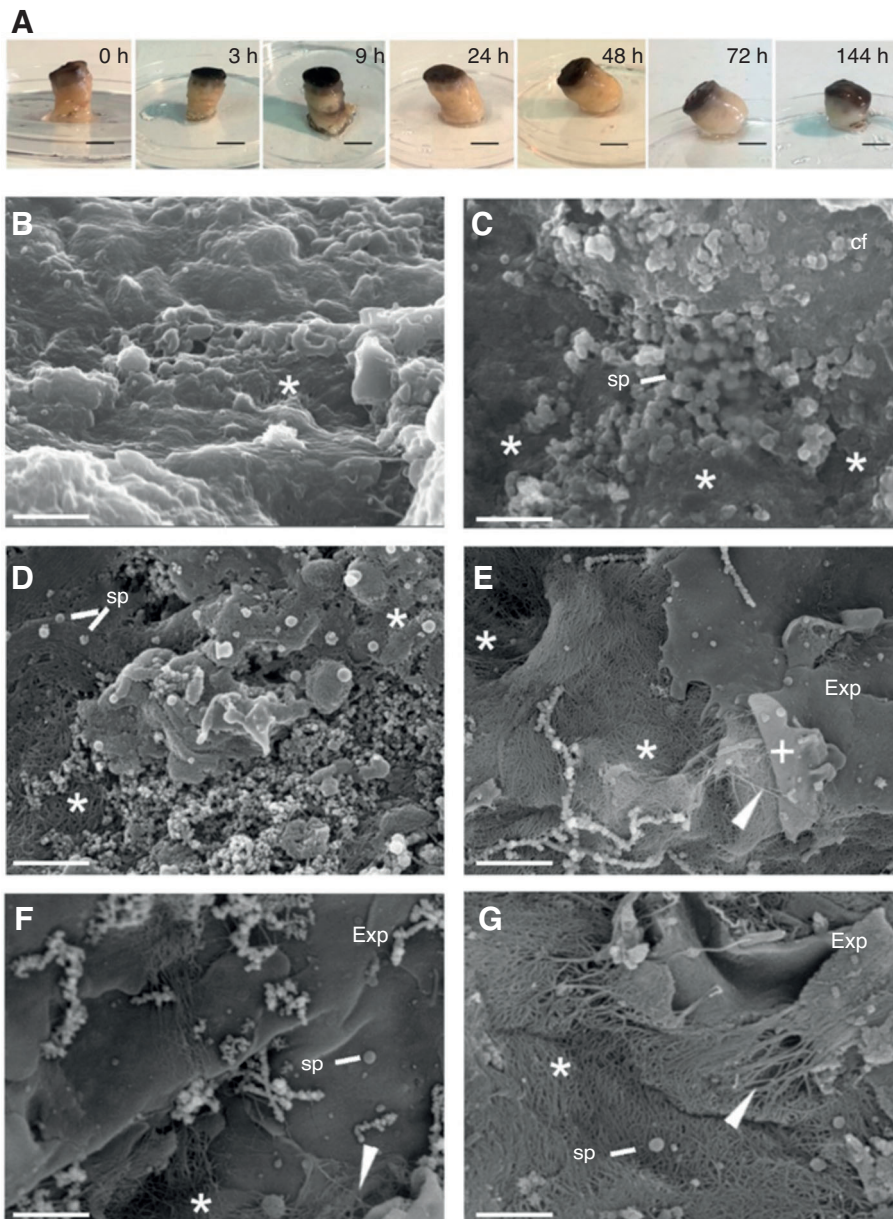


Fig. 2. Morphological modifications during sponge tissue regeneration. (A) Macroscopic morphological modifications of regenerating tissue explants (RTEs). Scale bars: 6 mm. (B–G) Ultrastructural SEM analysis of RTE wound surfaces at (B) 0 h, (C) 24 h, (D) 48 h, (E) 72 h and (F) 144 h post-excision. Scale bars: 2 μ m. (G) Another view of tissue at 144 h post-excision. Scale bar: 3 μ m. Asterisks, collagen bundles; arrowheads, collagen fibres; cf, cell fragments; ExP, exopinacocytes; sp, spherules.

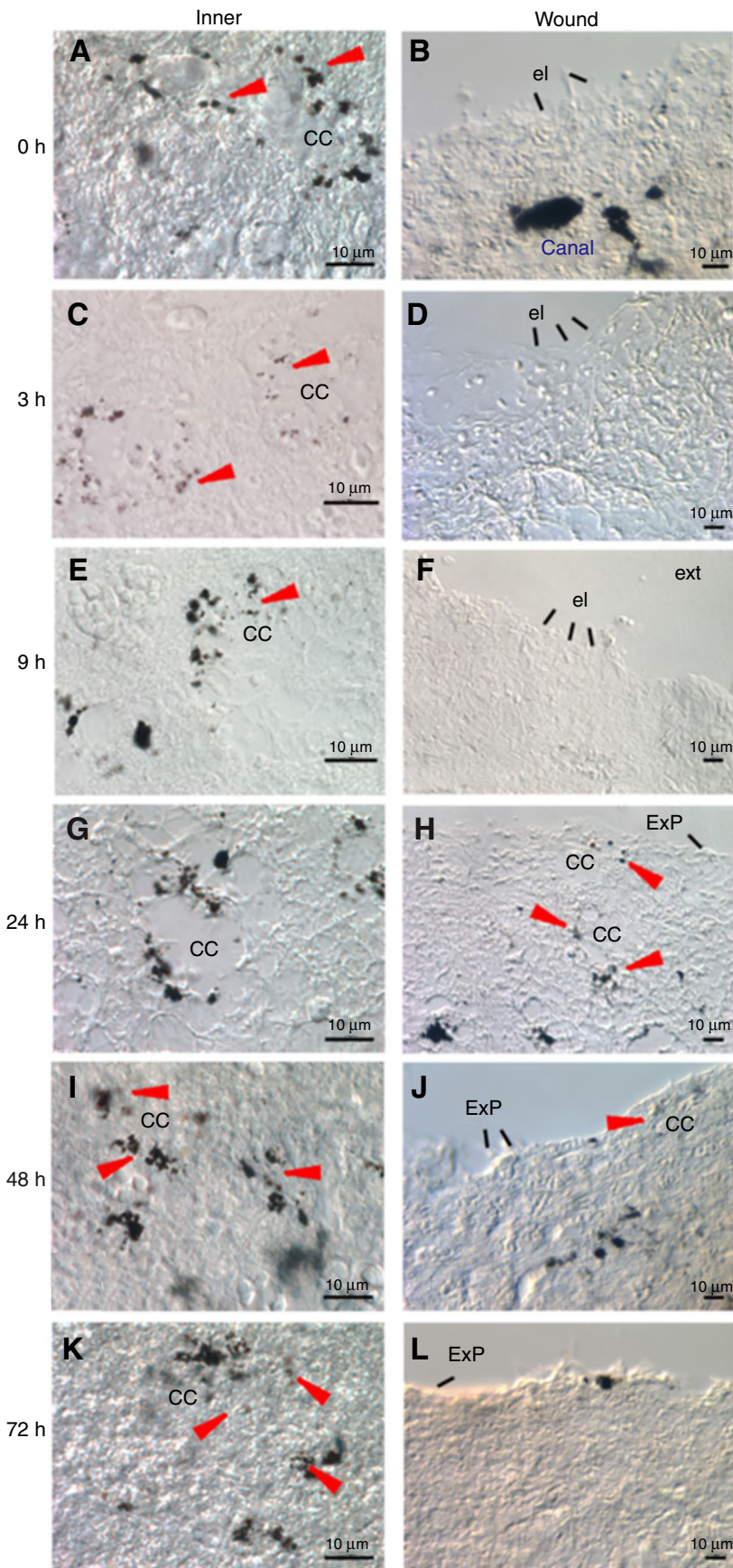


Fig. 3. Identification of choanocytes in *C. reniformis* RTEs. Transverse paraffin-embedded *C. reniformis* RTE sections pre-incubated with 2% India ink for 12 h. Micrographs show the RTE (A,C,E,G,I,K) inner region or (B,D,F,H,J,L) wound edge. Exp, exopinacocytes; CC, choanocyte chamber; el: external layer; red arrowheads: choanocytes; Canal: internal sponge canal. Scale bars: 10 µm.

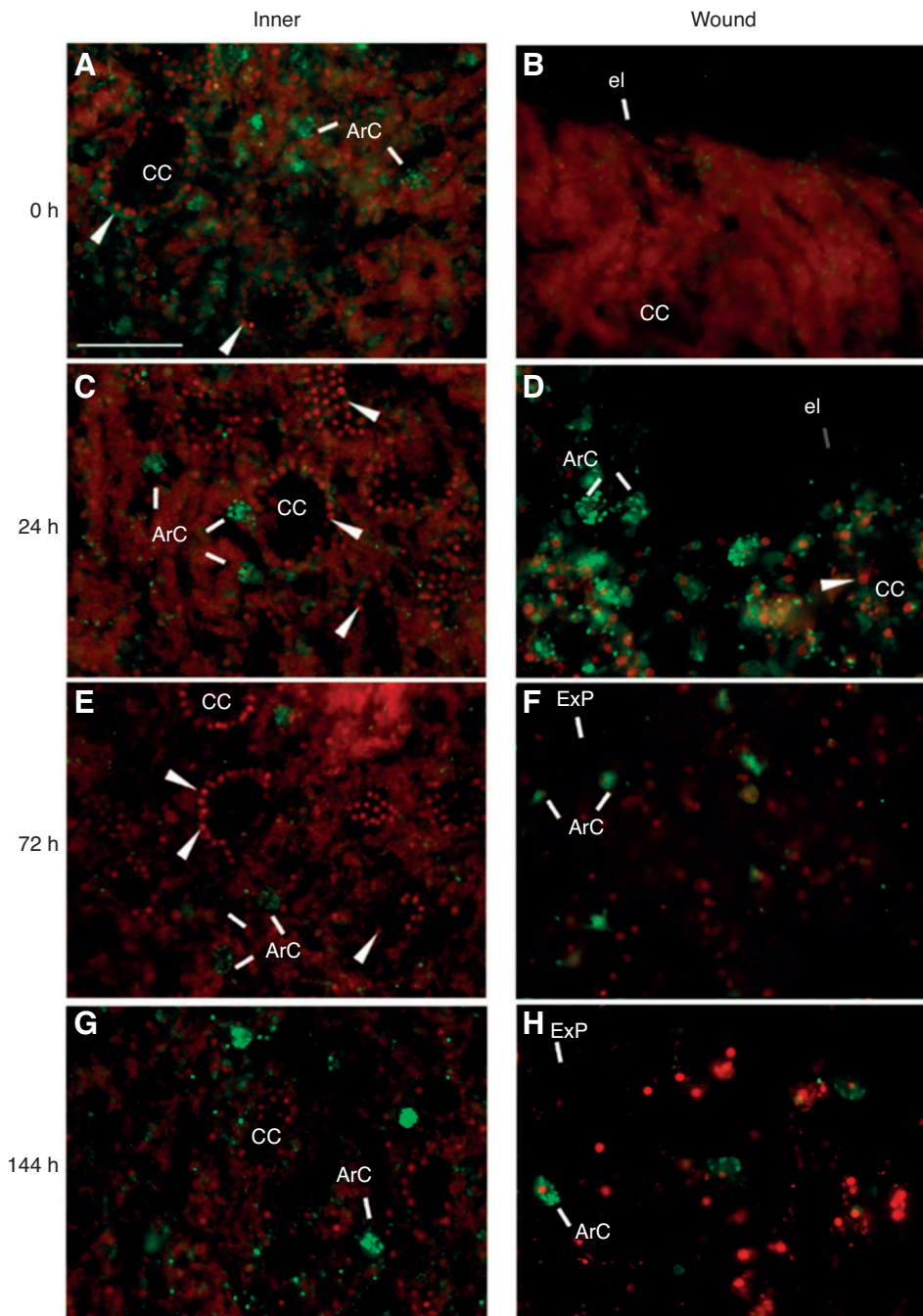


Fig. 4. Immunohistochemical identification of archeocytes in *C. reniformis* RTEs. Msi-1 immunofluorescence (green) and propidium iodide DNA staining (red) in RTEs. Micrographs show the RTE (A,C,E,G) inner region or (B,D,F,H) wound edge. Scale bars: 50 μ m. Arrowheads, choanocytes; CC, choanocyte chambers; ArC, archeocytes; el, external layer; Exp, exopinacocytes.

and debris, while the collagen fibres were less compact and a mesh-like structure was clearly visible (Fig. 2D, asterisks). Thin RTE sections from 48 h post-excision showed the presence of the first new exopinacocytes (Fig. 3J) that were not stained with India ink, a result that indicates these cells were not derived from choanocyte dedifferentiation.

Phase III, pinacocyte differentiation and exopinacoderm restoration (48–144 h)

Seventy-two hours after tissue excision, new exopinacocytes on the regenerating surfaces covering the collagen layer were observed (Fig. 2E). By 144 h after excision, these exopinacocytes had propagated from the collagen fibre mesh to completely cover the wound surface and restore the exopinacoderm (Fig. 2F,G).

Archeocyte immunostaining at the regenerating edge revealed a progressive Msi-1 signal reduction from 72 to 144 h after the wound (Fig. 4F and H, respectively), indicating a progressive archeocyte differentiation to new exopinacocytes.

Expression profile of stem-cell-regulating and anti-apoptotic genes

Piwi and Msi-1 help maintain pluripotent somatic stem cells (Glazer et al., 2012; Van Wolfswinkel, 2014), whereas Bcl-2 is an anti-apoptotic factor, and its downregulation is associated with an apoptotic state (Dejean et al., 2006).

Piwi expression did not show any change during the 144 h observation (Fig. 5A). *Msi-1*, however, was significantly upregulated at 9 and 24 h after excision, when it was possible to observe a fold increase of 1.55 ± 0.16 and 1.94 ± 0.58 compared with

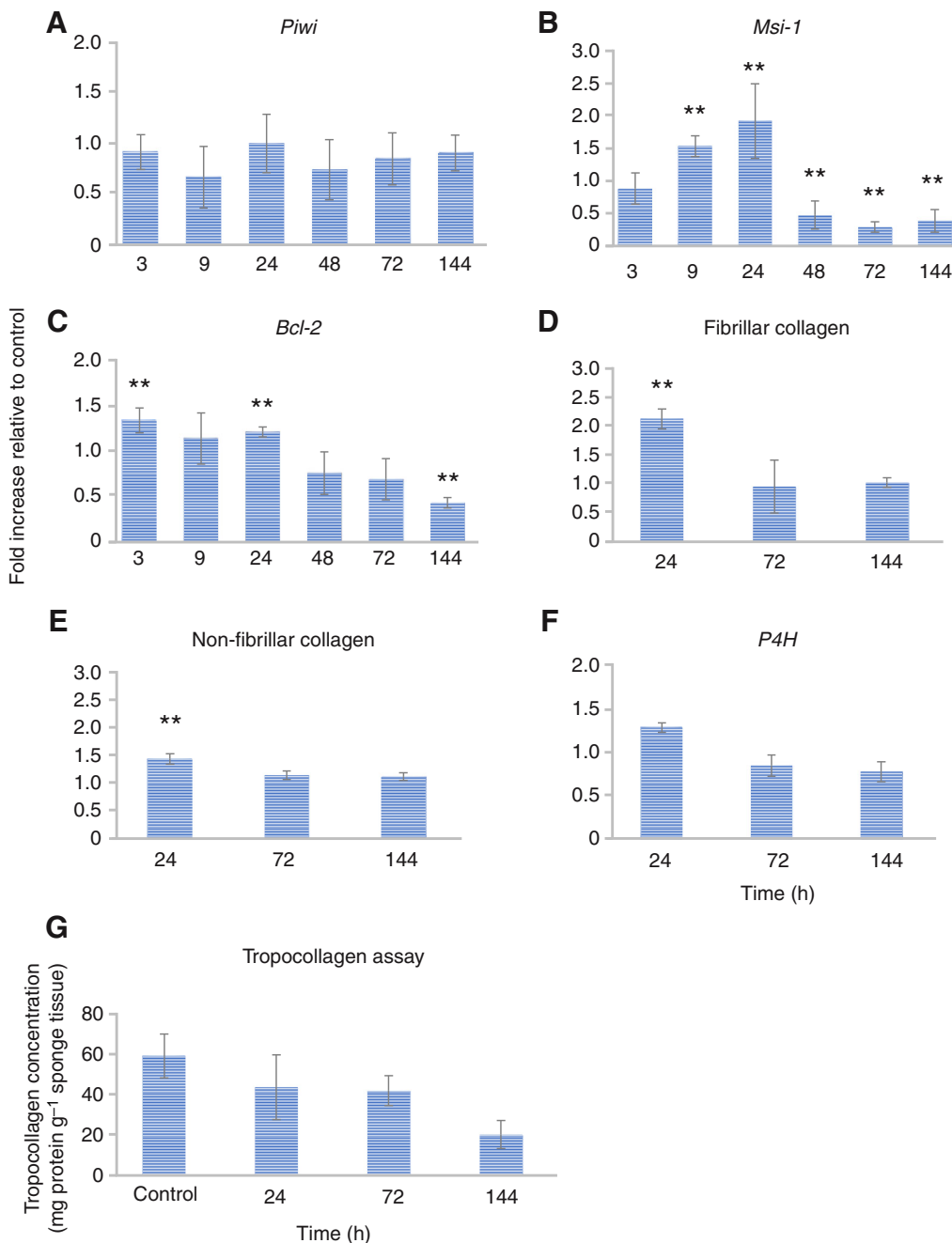


Fig. 5. Gene expression analysis of stem cell and anti-apoptotic genes during sponge tissue regeneration and fibrogenesis evaluation. qPCR gene expression analysis of stemness genes *Piwi* (A) and *Msi-1* (B), of the anti-apoptotic gene *Bcl-2* (C) and fibrogenic genes (D) fibrillar collagen, (E) non-fibrillar collagen and (F) *P4H*. Data are expressed as fold increase relative to the control and normalised to *GAPDH*. Each bar represents the mean \pm s.d. of three independent experiments performed in triplicate. Statistical analysis results: one-way ANOVA, $P=0.575521$ (A), $P<0.0001$ (B,C), $P<0.0001$ (D,E) and $P=0.018279$ (F). Asterisks indicate a significant difference versus the respective control (paired Tukey test, * $P<0.05$, ** $P<0.001$). (D) Salt-soluble tropocollagen quantification measured using the Sircol colorimetric method in *C. reniformis* RTEs. Each bar represents the mean \pm s.d. of three independent experiments performed in triplicate.

the control, respectively. From 48 to 144 h post-excision, *Msi-1* expression was downregulated compared with the control; the fold expression was 0.48 ± 0.21 , 0.29 ± 0.08 and 0.39 ± 0.17 at 48, 72 and 144 h, respectively (Fig. 5B). Because *Msi-1* upregulation is related to stem cell proliferation (Ishizuya-Oka et al., 2003), these results indicate archeocyte proliferating activity in the initial phase and cell differentiation afterwards.

Bcl-2 was slightly upregulated at 3 and 24 h post-excision, resulting in levels 1.36 ± 0.13 - and 1.23 ± 0.05 -fold higher than the control, respectively, but by 144 h its transcription was half that of the control (Fig. 5C).

Evaluation of fibrogenic activity

In order to establish whether sponge tissue regeneration is related to new collagen biosynthesis, we analysed fibrillar

collagen, non-fibrillar collagen and *P4H* gene expression. As shown in Fig. 5D, fibrillar collagen was significantly downregulated compared with the control until 72 h (except for the 9 h time point), and was strongly downregulated at 144 h post-excision (expression was 0.16 ± 0.12 -fold compared with the control). Non-fibrillar collagen was significantly downregulated during the entire exopinacoderm regeneration process (Fig. 5E). *P4H*, an enzyme involved in collagen post-translational modification, was downregulated at 3 and 144 h after excision but not significantly different at any other time point (Fig. 5F). In addition to the expression analysis of fibrogenic genes, we performed a total tropocollagen assay in RTEs. There were no significant differences in soluble tropocollagen at 24 or 72 h post-excision, whereas at 144 h it was one-third that of the control level (Fig. 5G).

TGF ligand and receptor gene expression profile during sponge exopinacoderm regeneration

We examined the gene expression of the six TGF ligands and two TGFrs identified in *C. reniformis* in 3, 9, 24, 48, 72 and 144 h-old RTEs. *TGF1* expression was only significantly different 144 h after tissue explant excision, when it was strongly downregulated to 0.15 ± 0.022 -fold with respect to the control level (Fig. 6A). *TGF2* expression did not change with respect to the control at any time point, a finding that suggests this TGF ligand is not directly involved in sponge tissue regeneration (Fig. 6B). *TGF3* was significantly downregulated beginning at 48 h. In detail, the *TGF3* mRNA fold expression was 0.33 ± 0.08 , 0.29 ± 0.12 and 0.45 ± 0.02 at 48, 72 and 144 h, respectively, compared with the control (Fig. 6C), indicating that the mRNA level of this TGF ligand decreases during the differentiation stage. *TGF4* was significantly upregulated at 72 and 144 h post-excision, being 4.4 ± 1.9 - and 4.6 ± 1.4 -fold higher than the control (Fig. 6D), data that suggest a possible role in

exopinacocyte differentiation as an antagonist to *TGF3*. *TGF5* was significantly upregulated compared with the control at all time points. In detail, at 3 and 9 h after the excision, the mRNA expression was 1.2 ± 0.11 - and 2.7 ± 0.67 -fold higher than the control, respectively. From 24 h on, a strong upregulation was detected, in particular a fold increase of 7.1 ± 3.3 , 5.8 ± 2.4 , 8.7 ± 3.3 and 6.7 ± 2.9 compared with the control was observed at 24, 48, 72 and 144 h post-excision, respectively (Fig. 6E). Conversely, *TGF6* was strongly upregulated during the early stages, namely until 24 h after the excision, showing a fold increase of 3.5 ± 1.4 , 10.2 ± 1.2 and 8.7 ± 0.76 with respect to the control at 3, 9 and 24 h, respectively, returning to control level at 48 and 72 h, and significantly downregulated at 144 h with a fold expression of 0.35 ± 0.27 with respect to the control (Fig. 6F).

TGFr1 and *TGFr2* were significantly downregulated at 3 h post-excision (Fig. 6G,H), with a fold expression of 0.62 ± 0.07 and 0.45 ± 0.09 compared with the control, respectively. Subsequently, at 9 h,

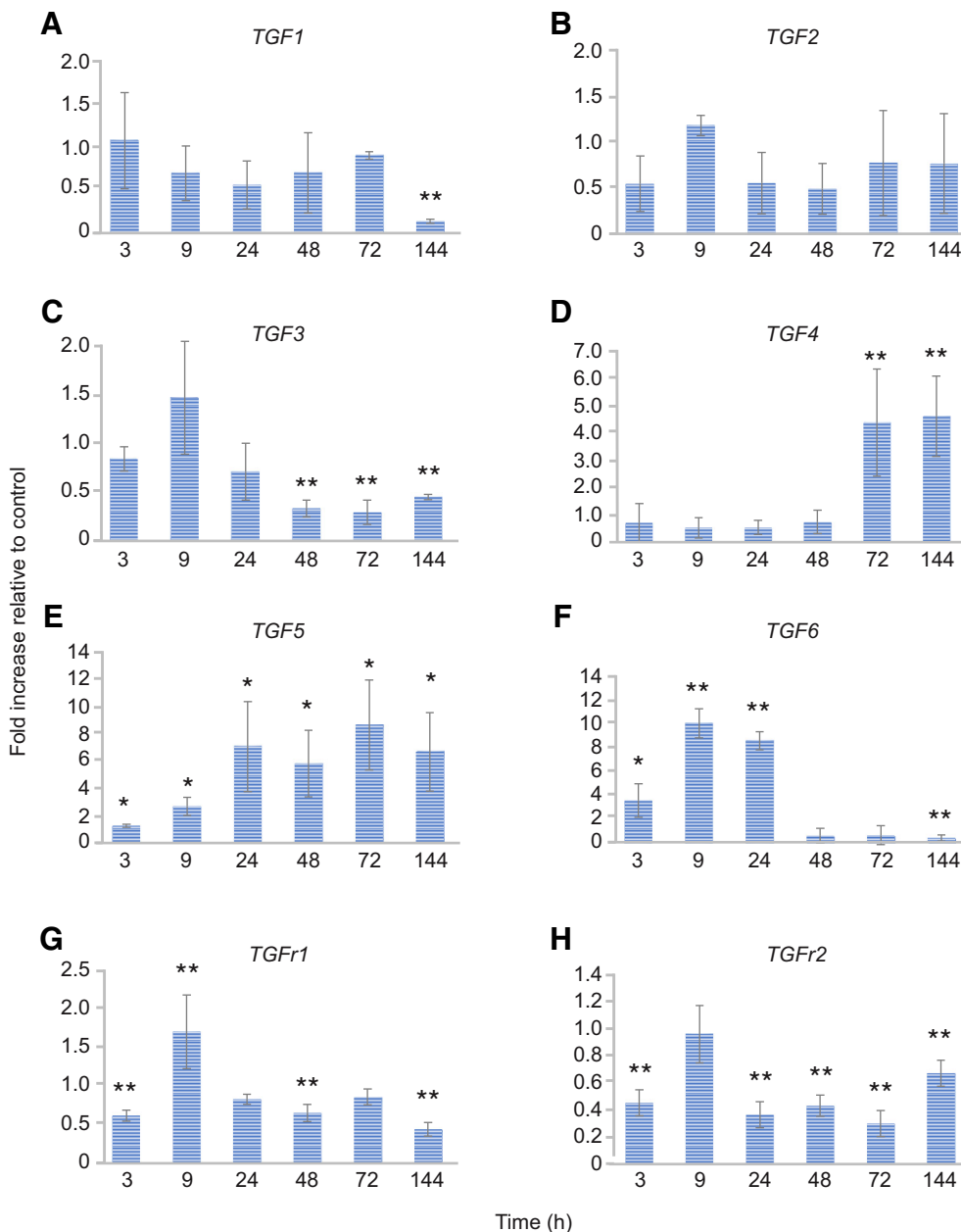


Fig. 6. Gene expression profile of TGF ligands and receptors during *C. reniformis* tissue regeneration. Gene expression for (A) *TGF1*, (B) *TGF2*, (C) *TGF3*, (D) *TGF4*, (E) *TGF5*, (F) *TGF6*, (G) *TGFr1* and (H) *TGFr2*. Data are expressed as fold increase relative to the control and normalised to *GAPDH*. Each bar represents the mean \pm s.d. of three independent experiments performed in triplicate. Statistical analysis results: one-way ANOVA, $P=0.045744$ (A), $P=0.247337$ (B) and $P<0.0001$ for all other genes. Asterisks indicate a significant difference versus the respective control (paired Tukey test, * $P<0.05$, ** $P<0.001$).

the *TGFr1* mRNA expression was 1.7 ± 0.4 -fold higher than that of the control; conversely, no significant variation in transcript amount was observed for *TGFr2* at the same time point. Further, *TGFr1* was significantly downregulated at 48 and 144 h (Fig. 6G), while *TGFr2* was significantly downregulated beginning at 24 h post-excision (Fig. 6H).

TGF6 mRNA tissue localisation was examined by *in situ* hybridisation on histological sections derived from whole-animal (0 h) and from 24- and 72-h-old RTE sections. *TGF6* signal was detected around the CCs, and thus choanocytes were the cellular source of this gene (Fig. 7A). Although this approach cannot provide quantitative information with regards to signal intensity, the comparison between the 24 and 72 h post-excision samples (Fig. 7B and C, respectively) with the whole animal (Fig. 7A) allowed us to infer that the remarkable increase in *TGF6* mRNA during the first 24 h was due to a gene upregulation in a defined number of choanocytes rather than an overall higher number of cells producing *TGF6*.

TGF inhibitor effect

RTEs were incubated with 0.1 mmol l^{-1} SB431542, a potent TGF- β inhibitor. Morphological observations at the macroscopic level indicated that at 144 h post-excision, the RTEs incubated with SB431542 were visibly less rounded than the untreated control (Fig. 8A). Ultra-structurally, the regenerating surfaces of TGF- β -inhibitor-treated RTEs at 24 h indicated frayed and less compact collagen fibres with a wider mesh than the control (Fig. 8B,C). At 72 and 144 h after the cut, control samples showed visible new exopinacocytes that covered the wound surface (Fig. 8D,F), but these cells were absent with TGF- β inhibitor treatment (Fig. 8E,G). The lack of the exopinacoderm layer and the reduced, disorganised collagen fibres in the 144-h SB431542-treated RTEs was confirmed by MT staining (Fig. 8H,I). Furthermore, PSR staining revealed a marked reduction in collagen fibre diameter in inhibitor-treated RTEs (Fig. 8K).

We next examined whether TGF ligands were involved in the proliferation/differentiation activity, apoptosis and fibrogenesis inhibition observed in sponge regeneration by evaluating *Msi-1*, *Bcl-2*, fibrillar and non-fibrillar collagen, and *P4H* expression in RTEs exposed to the TGF- β inhibitor. As previously shown, *Msi-1* was significantly upregulated at 9 and 24 h post-excision, attesting to a proliferative state of the archeocytes (Fig. 5B), followed by downregulation as archeocytes differentiated to exopinacocytes. At 24 h post-excision, SB431542 treatment further upregulated *Msi-1* by 2.24 ± 0.33 -fold compared with the untreated control, but there was no difference between treated and control RTEs at 72 or 144 h (Fig. 9A). These data suggest that the TGF- β inhibitor could antagonise a TGF ligand that, at 24 h, starts to reduce the proliferative state in order to drive the differentiation stage. SB431542 treatment did not alter *Bcl-2* expression at any time point, suggesting TGF ligands are not directly involved in apoptosis during sponge tissue regeneration (Fig. 9B). Fibrillar and nonfibrillar collagen were both significantly upregulated at 24 h post-excision in inhibitor-treated compared with the control RTEs. However, there were no expression changes at later time points (Fig. 9C).

DISCUSSION

Elucidating the molecular pathways of tissue regeneration in lower metazoans may help reconstruct the evolutionary history of the genes involved in this important adaptive response. Because marine sponges (Porifera) were among the earliest branching Animalia phyla, they represent an extremely informative experimental model for this purpose. TGF superfamily members are a class of secreted proteins involved in morphogenesis and wound healing in most metazoans (Barrientos et al., 2008). Thus, this work aimed to establish the involvement of these molecules in sponge tissue regeneration by analysing their expression pattern during the regeneration process.

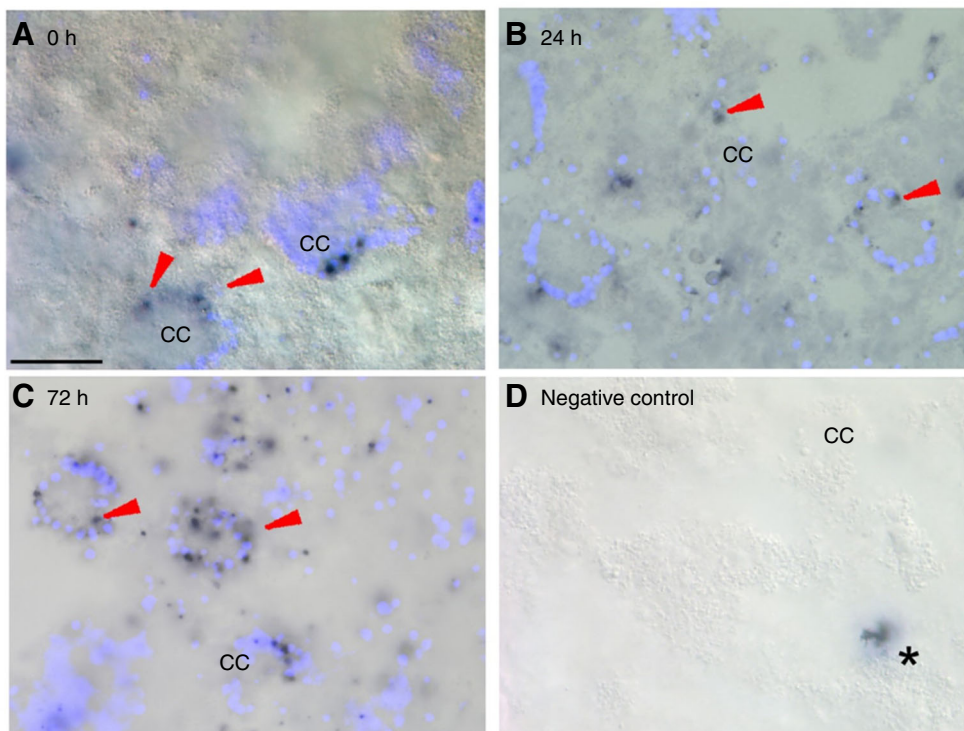


Fig. 7. *TGF6* transcript *in situ* hybridisation analysis in RTEs. Positive *TGF6* signal at (A) 0 h, (B) 24 h and (C) 72 h post-excision. (D) Negative control. Red arrowheads, choanocyte chambers; asterisk, non-specific precipitate. Nuclei were counterstained with DAPI. Scale bar (applies to all panels): 200 μm .

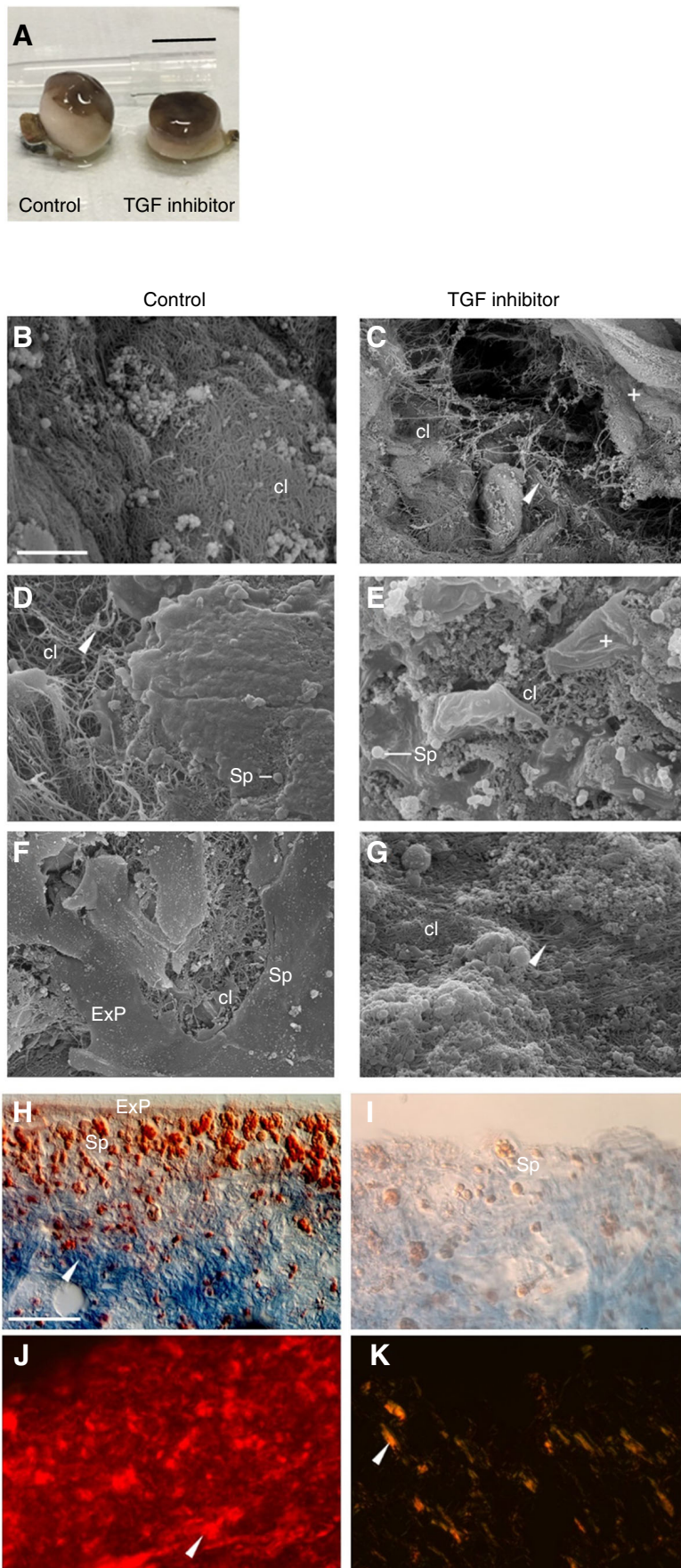


Fig. 8. Morphological analysis of RTEs treated with a TGF inhibitor. (A) 144 h-old sponge explants regenerating in the absence (left) or presence (right) of a TGF inhibitor (0.1 mmol l^{-1} SB431542). Scale bar: 6 mm. (B–G) SEM images of the cut surface at 24 h (B, C), 72 h (D, E) and 144 h (F, G) post-excision for untreated (Control; B, D and F, respectively) and 0.1 mmol l^{-1} SB431542-treated RTEs (C, E and G, respectively). Scale bar: $2.5 \mu\text{m}$. (H–K) Paraffin sections of (H, J) 144-h-old untreated RTEs and (I, K) RTEs incubated in the presence of 0.1 mmol l^{-1} SB431542. Sections were stained with Masson's Trichrome (H, I) or Picro Sirius Red (J, K). Scale bar: $10 \mu\text{m}$. cl, exposed collagen; +, cell fragment; arrowhead, large-diameter collagen fibres; ExP, exopinacocyte; Sp, spherules.

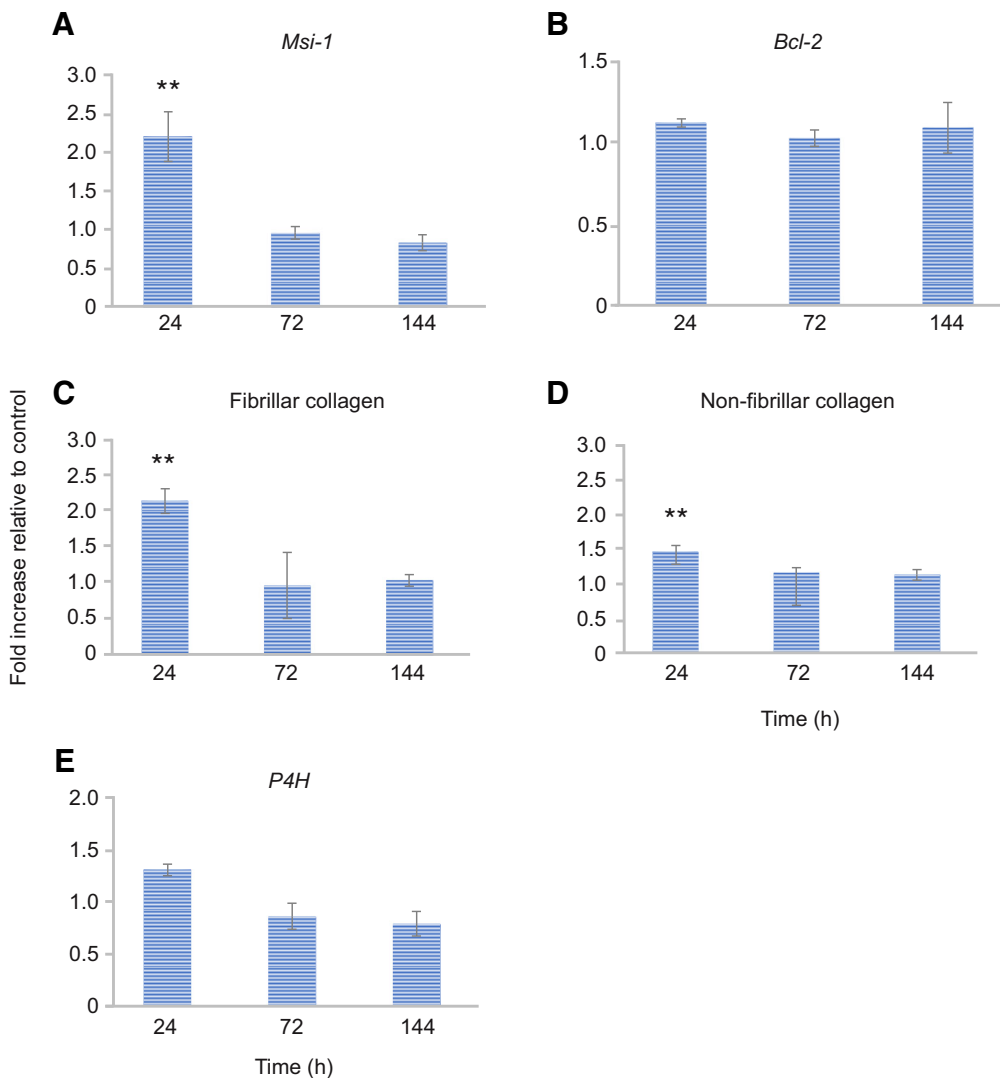


Fig. 9. Gene expression of *Msi-1*, *Bcl-2* and fibrogenic genes in RTEs treated with a TGF inhibitor. qPCR expression of (A) stemness gene *Msi-1*, (B) anti-apoptotic gene *Bcl-2*, (C) fibrillar collagen, (D) non-fibrillar collagen and (E) *P4H* in RTEs in the presence of 0.1 mmol l^{-1} SB431542 for 24, 72 or 144 h. Data are expressed as fold increase relative to the control (untreated sample) and normalised to *GAPDH*. Each bar represents the mean \pm s.d. of three independent experiments performed in triplicate. Statistical analysis results: one-way ANOVA, $P < 0.0001$ (A), $P = 0.340350$ (B), $P < 0.001$ (C), $P < 0.001$ (D) and $P < 0.0005$ (E). Asterisks indicate a significant difference versus the respective control (paired Tukey test, * $P < 0.05$, ** $P < 0.001$).

Owing to the already documented involvement of some TGF superfamily members in extracellular matrix deposition during wound healing and scarring in higher animals (O'Kane and Ferguson, 1997), these growth factors are among the most interesting targets for the study of the molecular mechanisms coordinating tissue restoration in these low metazoans characterized by highly fibrous bodies.

The experimental model selected for the present study was the demosponge *C. reniformis* owing to the ability of its tissue explants to completely regenerate the exopinacoderm layer in a controlled system (Pozzolini et al., 2012).

We identified seven TGF-ligand- and three receptor-coding transcripts in the *C. reniformis* transcriptome. However, two ligands and two receptors were presumably derived from alternative splicing of the same gene (Table S1). Notably, the number of identified transcripts was lower compared with those found in *A. queenslandica* and *M. leidy*, where there were eight and nine TGF ligands and five and four TGFrs, respectively (Pang et al., 2011). This discrepancy may be explained by different experimental techniques. In the latter models, the transcripts were identified from the genome, and hence we cannot exclude that there could be other *C. reniformis* genes that may not be transcribed in the adult organism (from which the transcriptome was prepared). Indeed,

transcriptomes from adult *A. vastus*, *C. nucula*, *C. candelabrum*, *I. fasciculata*, *P. ficiformis*, *P. suberitoides* (Riesgo et al., 2014) and *H. caerulea* (Kenny et al., 2018) sponges generally included fewer TGF ligands and receptors than *A. queenslandica* (Tables S2 and S3). Multiple alignments among TGF- β peptides deduced from the identified TGF ligands with TGF- β peptide derived from human TGF- β revealed that, except for *TGF1* and *TGF2*, all seven cysteine residues were maintained within the TGF domain. These results demonstrate that this region is more conserved compared with TGF domains present in the nine TGF ligands identified in the phylum Ctenophora (Pang et al., 2011). As previously reported in sponges for the TNF/TNF-receptor (Pozzolini et al., 2016a,b), and now here, in the TGF/TGF-receptor system, the receptors share greater homology with their corresponding counterparts in higher Metazoa than the ligands. This observation further confirms increased evolutionary constraints on intracellular molecular components compared with extracellular counterparts. The variations in number and sequences of the TGF ligands compared with the receptors and components involved in intracellular signal transduction (e.g. SMAD proteins) may be due to the reuse of the same intracellular molecular machinery for different extracellular modulators (Herpin et al., 2004). Therefore, in *C. reniformis* as well as in higher animals, it is possible that the seven TGF ligand types

can be selectively recognised by only three different receptor types owing to fine modulation of subunit combinations.

The phylogenetic placement of *C. reniformis* TGF superfamily members (Fig. S3A), using the same data set utilised by Pang et al. (2011), revealed that sponge TGF ligands do not group into any of the TGF clades. When including various putative TGF-like molecules derived from other sponge species (Table S3), this result is reinforced, a finding that indicates that during sponge evolution, various TGF paralogues probably originated independently to mediate sponge-specific functions. The only exception was for a TGF transcript derived from *C. candelabrum* that grouped into the TGF- β clade. These data confirm that although all bilaterian animals have at least one gene from the TGF- β , all non-bilaterians, except sponges, have at least one member from the BMP-like group (Pang et al., 2011). It is not surprising that the only TGF-like transcript grouped into the TGF- β clade is derived from a member of the Homoscleromorpha, as this class represents the most evolved sponges (Wörheide et al., 2012). They are the only sponge class with a basal membrane (similar to higher animals), and therefore its TGF- β -like ligand could be involved in the Wnt pathway, perhaps in ectoderm development. Phylogenetic analysis of TGFs revealed that all the identified transcripts were grouped into the Type I TGF receptor clade. Thus, Type I receptors appear to prevail in sponges. In our study, the only sponge TGFr grouped into the Type II clade were from *A. queenslandica*. Because data from this species were derived from the genome, it is possible that the Type II sponge TGFr is expressed only during the larval stage and could not be identified in the adult transcriptomes of the other sponges. Transcripts coding for a Type II TGFr were described in the freshwater sponge *Ephydatia fluviatilis*; these sequences were identified from a cDNA library derived from the gemmules, one of the sponge asexual reproduction systems comparable to the larval system (Tanaka and Watanabe, 1984).

We studied *C. reniformis* exopinacoderm restoration in tissue explants over 144 h. The regeneration process presented three

phases: (i) archeocyte proliferation; (ii) archeocyte migration/differentiation; and (iii) exopinacocyte layer restoration (Fig. 10). As previously reported by Nickel and Brümmer (2003), after initial swelling, the tissue fragments gradually became rounded and compact over 144 h. Compared with the wound healing process described in the genus *Halisarca* (Alexander et al., 2015; Borisenko et al., 2015), except for the initial steps (at 3 and 9 h after excision, when cell debris and mucus are released from the edge of the cut), *C. reniformis* tissue regeneration was slower. Indeed, whereas the exopinacoderm was restored within 24 h in *Halisarca*, in our experimental conditions the first exopinacocytes were identified in the wound area after 48–72 h. This temporal discrepancy may be due to the different experimental model used rather than interspecific variability in morphogenetic activity. While ultrastructural studies in *Halisarca* were performed on whole specimens in a small area, we analysed regeneration in a large number of identical RTEs, where the choanosome/ectosome ratio is markedly different compared with previous studies. Sponges maintain considerable proliferative activity even as adults owing to their pluripotent stem cell pool as indicated by their high tissue telomerase activity (Pozzolini et al., 2014). Funayama (2010) proposed that the stem cell system in demosponges is composed of both archeocytes and choanocytes and that the proteins Piwi and Musashi are primarily responsible for proliferative cell maintenance. In particular, although *Piwi* is expressed in both archeocytes and choanocytes, *Msi-1* seems to be specific for archeocytes (Okamoto et al., 2012). In our experimental model, the exopinacocyte layer resulted from differentiation of archeocytes that migrated from the mesohyl (Fig. 2D,E), while specific India ink choanocyte staining (Fig. 3) excluded any involvement of this cell type in the regeneration process. This exclusion differed from *Halisarca* regeneration (Borisenko et al., 2015). This observation was supported by *Piwi* and *Msi-1* gene expression (Fig. 5A,B). While *Piwi* mRNA did not change during the regeneration process, *Msi-1* was first upregulated at 9 and 24 h after tissue excision and

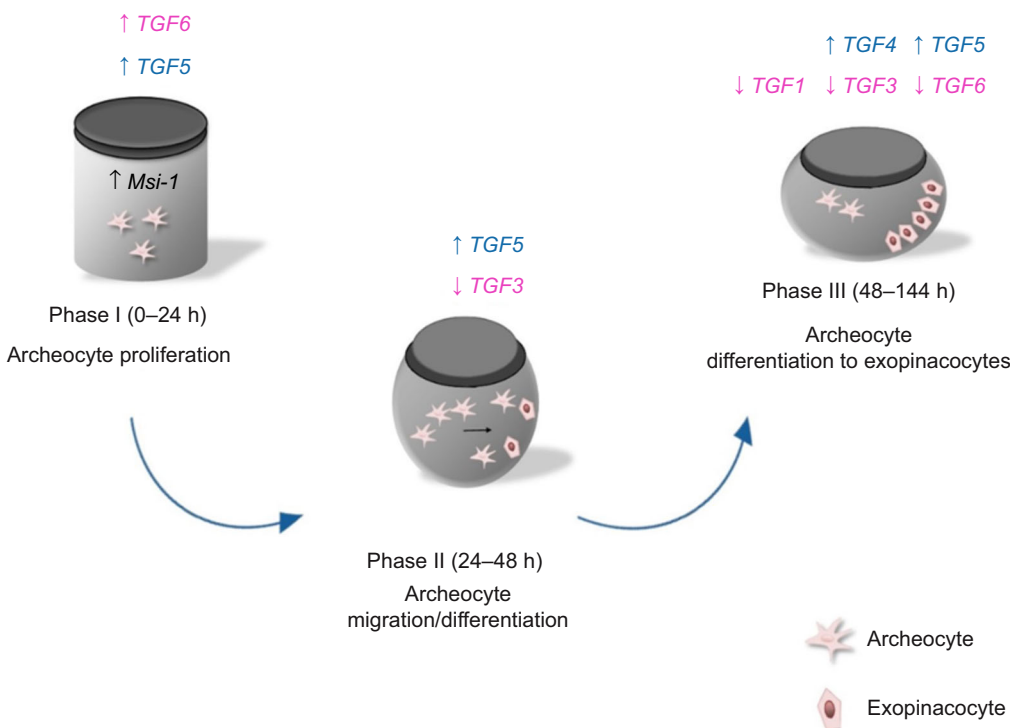


Fig. 10. Summary diagram of the TGF ligand expression profile and the possible role of TGFs in *C. reniformis* exopinacoderm regeneration. Phase I (0–24 h): *TGF5* and *TGF6* are upregulated; *Msi-1* upregulation indicates archeocyte proliferation. Phase II (24–48 h): *TGF5* is upregulated while *TGF3* is downregulated, and there is archeocyte migration to the wound area. Phase III (48–144 h): archeocytes progressively differentiate into new pinacocytes. *TGF4* and *TGF5* are upregulated, indicating involvement in the differentiation; *TGF1*, *TGF3* and *TGF6* are downregulated and likely contribute to maintaining the proliferative state. Blue-lettered molecules indicate potential pro-differentiating growth factors, while pink-lettered molecules indicate potential stemness-inducing effectors.

then significantly decreased after 48 h. The lack of significant variation of the *Piwi* mRNA level may be explained by the maintenance of the expression of this gene also in differentiated choanocytes, hence we may not have observed a change in this mRNA level in the regeneration edge that contained abundant choanocytes. In view of this, the tracking of *Msi-1* expression with respect to that of *Piwi* in our experimental model is more accurate and informative as *Msi-1* expression is exclusive to archeocytes. Notably, *Msi-1* upregulation during early regeneration is indicative of increased cell proliferation, as previously reported in the same model (Nickel and Brümmer, 2003). In higher animals, *Msi-1* is also upregulated in stem cell proliferating systems (Glazer et al., 2012; Ishizuya-Oka et al., 2003). The decrease of *Msi-1* gene expression after 48 h suggests a progressive differentiation from archeocytes to new exopinacocytes (Okamoto et al., 2012).

The expression of all TGF ligands, except for *TGF2*, significantly changed during sponge tissue regeneration, data that indicate their possible involvement in the process. Their expression is characterised by temporal variation that suggests an antagonistic activity among the different TGFs. As shown in Fig. 10, during the first 24 h post-excision, *TGF6* was strongly upregulated, indicating its possible involvement in archeocyte proliferation by means of *Msi-1* gene upregulation (Fig. 5B). Comparatively, *TGF4* was only altered (upregulated) at 72 h after excision, namely during archeocyte differentiation into exopinacocytes (Fig. 2E), a change suggestive of involvement in this differentiation step. *TGF5* was upregulated over the entire 144 h observation period. It is possible that while *TGF6* acts as a pro-stemness factor, *TGF4* and *TGF5* could act as pro-differentiating factors. *TGF1* and *TGF3* were downregulated during late regeneration and, like *TGF6*, they may be involved in maintenance of the stem cell state. The relative mRNA content of the six TGF ligands in the whole animal (Fig. 1) supports this hypothesis. Indeed, in the steady-state sponge, when proliferation is physiologically high (Pozzolini et al., 2014), *TGF6* is expressed 20-fold more than *TGF4*, while *TGF1* and *TGF3* are expressed 50- and 20-fold higher, respectively, than *TGF4*. Thus, *TGF4* and *TGF5* expression apparently increases only during sponge tissue regeneration. Overall, *TGF1*, *TGF3* and *TGF6* could have pro-stemness activity because their expression is highest in the intact sponge and decreases during sponge regeneration. Conversely, *TGF4* and *TGF5* could serve as pro-differentiating factors because their expression is highest in the differentiation phase of the tissue regeneration. The antagonistic behaviour among various TGF superfamily members on transition from an undifferentiated to a differentiated state is maintained also in higher animals, where *TGFβ* signalling by activin A and *TGF-β* itself is supportive of the undifferentiated state in human embryonic stem cells (James et al., 2005) while BMPs are strongly involved in osteoblast differentiation (Scarfi, 2016).

During sponge exopinacoderm regeneration, *TGF6* was the most upregulated of all ligands (10-fold compared with the control), specifically between 9 and 24 h post-excision. This mRNA was almost exclusively derived from choanocytes (Fig. 7). As described by Alexander et al. (2015), adult sponges rapidly renew their filter system by maintaining highly proliferative choanocytes. Therefore, it is not surprising to find the pro-stemness effector *TGF6* highly expressed in these cells. Although the choanocytes in our model were not directly involved in exopinacoderm restoration, these cells secreted *TGF6*, and this cytokine is the main candidate also for archeocyte proliferation induction. Furthermore, the high *TGF6* level in the adult sponge (Fig. 1), combined with its tissue localisation only in choanocytes, strongly suggests that *TGF6*

participates in the renewal of the sponge filtering system by inducing choanocyte proliferation.

In order to functionally confirm the involvement of TGF ligands in sponge tissue regeneration, RTEs were incubated in the presence of a specific TGF inhibitor (SB431542). We chose this inhibitor because all identified TGFs were grouped into the Type I clade. This compound selectively inhibits *alk5/TGF-β* type I receptor activity (Inman et al., 2002), and it also inhibits TGF ligands in Ctenophora larvae (Pang et al., 2012). In our model, at 144 h post-excision, the inhibitor-treated RTEs appeared visibly less rounded than the untreated controls (Fig. 8A). Ultrastructural analysis indicated that, in presence of SB431542, sponge exopinacoderm restoration failed (Fig. 8G), a result that confirms the involvement of the TGF pathway in this process. Moreover, in the presence of the TGF inhibitor, *Msi-1* gene expression significantly increased compared with untreated control, albeit only 24 h after the tissue excision and not over longer time periods. This behaviour could be explained by considering a possible antagonistic activity between *TGF5* and *TGF6*. The proliferative state of the sponge stem cell system may be regulated by a fine balance of the complementary activity of these two factors, and the progressive *TGF5* increase could drive differentiation while reducing *TGF6*-mediated proliferation. SB431542 treatment possibly selectively impaired *TGF5* signal transduction and caused an imbalance toward *TGF6*-mediated proliferation. Because *Msi-1* expression was not different between SB431542-treated and untreated samples during later regeneration, *TGF4* could restore the correct proliferative/differentiative balance. However, this compensation is not sufficient to avoid TGF-inhibitor-mediated exopinacoderm restoration inhibition. Apparently, the inhibition of factors that act during early regeneration affects subsequent stages. These TGF-inhibitor-induced changes suggest that it particularly impairs *TGF5* signal transduction. Thus, it is possible that the *TGF5*–*TGF* system is more closely related to the SB431542 target in higher Metazoa compared with the other ligands.

Regeneration and morphogenetic processes may involve apoptosis (Bergmann and Steller, 2010) as well as extracellular matrix remodelling (Daley et al., 2007). In higher animals, *TGF-β* can act as a survival factor by modulating *Bcl-2* expression (Grzelkowska et al., 1998). In our model, *Bcl-2* was slightly upregulated at 3 and 24 h post-excision and downregulated at 144 h, data that suggest that apoptosis occurs during the final stage of exopinacoderm restoration (Fig. 5C). This behaviour could be explained as a response of the aquiferous system reorganization by the closure or streamlining of some canal and choanocyte elimination. In the presence of SB431542, however, *Bcl2* expression was no different compared with the untreated control at any time point. This suggests that although *TGF5* may not be involved in apoptosis induction, the possible involvement of other TGF ligands may not be excluded. Surprisingly, during *C. reniformis* tissue regeneration we observed a significant downregulation of fibrillar and non-fibrillar collagen genes combined with a reduction in tropocollagen content (Fig. 5G). This behaviour is opposite of what was described for *H. caerulea* wound healing, where PSR staining indicated increased collagen density in the wounded area (Alexander et al., 2015). Nevertheless, it is necessary to consider the peculiar structure of the *C. reniformis* choanosome, which results in extremely dense and thick collagen fibres. The reduction in fibrogenesis during tissue regeneration could facilitate the migration of archeocytes through the packed collagen fibres to reach the wounded area (Fig. 2G). This supposition would also explain the RTE swelling during early

tissue regeneration. Moreover, during regeneration, it may be necessary to reduce the energetically expensive fibrogenesis in favour of new exopinacoderm formation. This trade-off was observed in *Halisarca*, where normal choanocyte renewal was momentarily blocked near the healing area, presumably to economise the biochemical activities (Alexander et al., 2015). Fibrillar and non-fibrillar collagen genes were upregulated in TGF-inhibitor-treated RTEs compared with the control only at 24 h post excision, data that implicate a contribution of TGF ligands to collagen biosynthesis inhibition, at least during early sponge tissue regeneration. This behaviour is opposite of that observed in higher animals, where many TGF superfamily members usually act as fibrogenic agents under physiological conditions (Piek et al., 1999) and wound healing (Barrientos et al., 2008). It is possible that although in the higher organisms the various TGF paralogues have evolved to drive similar pathways in various tissues (e.g. bone and cartilage), in the relatively primitive sponges that lack well-organised tissues and organs, the TGF paralogues could still drive antagonistic functions such as proliferation/differentiation or fibrogenesis/collagen degradation. The prevailing condition would be the one that exerts the greatest activity.

Taken together, these observations indicate that TGF superfamily members in sponges are involved in wound healing, mainly driving the mesenchymal–epithelial transition, a finding that reveals that this growth factor class have maintained this functional specialisation during evolution; in contrast, in relation to collagen deposition and scarring, in our experimental conditions the TGF superfamily members exhibited an opposite behaviour with respect to that in higher animals. The data also confirm that TGFs are part of the molecular toolkit that control tissue regeneration that is conserved across the tree of life. Beyond these phylogenetic considerations, the identification of pro-differentiating and pro-stemness humoral factors, as well as of agents capable of controlling the fibrogenesis state, provides intriguing implications for this sponge in biotechnological applications of collagen-derived biomaterials.

Acknowledgements

The authors are indebted to Laura Negretti for her excellent technical support in ESEM analyses, and to Cristina Gagliani and Katia Cortese for TEM analysis.

Competing interests

The authors declare no competing or financial interests.

Author contributions

Conceptualization: M.P., S.S.; Methodology: M.P., L.G., S.F., S.C., M. Bozzo, G.C.; Software: S.G.; Investigation: M.P., L.G., S.F., S.G., M. Bozzo; Resources: L.G., S.F., M. Bertolino, G.B.; Data curation: L.G., M. Bertolino, G.B.; Writing - original draft: M.P.; Writing - review & editing: S.C., S.S.; Supervision: G.B., S.S.; Funding acquisition: M.P., M. Bertolino, S.S.

Funding

This work was supported by University of Genova funding to both S.S. and M.P., and by Scientific Independence of Young Researchers (SIR) funding through the Italian Ministry of University and Research (MIUR) to M.Be.

Supplementary information

Supplementary information available online at <http://jeb.biologists.org/lookup/doi/10.1242/jeb.207894.supplemental>

References

- Aarskog, N. K. and Vedeler, C. A. (2000). Real-time quantitative polymerase chain reaction. A new method that detects both the peripheral myelin protein 22 duplication in Charcot-Marie-Tooth type 1A disease and the peripheral myelin protein 22 deletion in hereditary neuropathy with liability to pressure palsies. *Hum. Genet.* **107**, 494–498. doi:10.1007/s004390000399
- Adamska, M., Degnan, S. M., Green, K. M., Adamski, M., Craigie, A., Larroux, C. and Degnan, B. M. (2007). Wnt and TGF-beta expression in the sponge *Amphimedon queenslandica* and the origin of metazoan embryonic patterning. *PLoS ONE* **2**, e1031. doi:10.1371/journal.pone.0001031
- Alexander, B. E., Mueller, B., Vermeij, M. J. A., van der Geest, H. H. G. and de Goeij, J. M. (2015). Biofouling of inlet pipes affects water quality in running seawater aquaria and compromises sponge cell proliferation. *Peer J* **3**, e1430. doi:10.7717/peerj.1430
- Barrientos, S., Stojadinovic, O., Golinko, M. S., Brem, H. and Tomic-Canic, M. (2008). Growth factors and cytokines in wound healing. *Wound Rep. Reg.* **16**, 585–601. doi:10.1111/j.1524-475X.2008.00410.x
- Bergmann, A. and Steller, H. (2010). Apoptosis, stem cells, and tissue regeneration. *Sci. Signal.* **3**, re8. doi:10.1126/scisignal.3145re8
- Borisenko, I. E., Adamska, M., Tokina, D. B. and Ereskovsky, A. V. (2015). Transdifferentiation is a driving force of regeneration in *Halisarca dujardini* (Demospongiae, Porifera). *PeerJ* **3**, e1211. doi:10.7717/peerj.1211
- Candiani, S., Garbarino, G. and Pestarino, M. (2015). Detection of mRNA and microRNA expression in basal chordates, amphioxus and ascidians. *Neuromethods* **99**, 279–292. doi:10.1007/978-1-4939-2303-8_14
- Custodio, M. R., Prokic, I., Steffen, R., Kozioł, C., Borojevic, R., Brummer, F., Nickel, M. and Müller, W. E. G. (1998). Primmorphs generated from dissociated cells of the sponge *Suberites domuncula*: a model system for studies of cell proliferation and cell death. *Mech. Ageing Dev.* **105**, 45–59. doi:10.1016/S0047-6374(98)00078-5
- Daley, W. P., Peters, S. B. and Larsen, M. (2008). Extracellular matrix dynamics in development and regenerative medicine. *J. Cell Sci.* **121**, 255–264. doi:10.1242/jcs.006064
- Dejean, L. M., Martinez-Caballero, S., Manon, S. and Kinnally, K. W. (2006). Regulation of the mitochondrial apoptosis-induced channel, MAC, by BCL-2 family proteins. *Biochim. Biophys. Acta* **1762**, 191–201. doi:10.1016/j.bbadis.2005.07.002
- Ereskovsky, A. V., Borisenko, I. E., Lapébie, P., Gazave, E., Tokina, D. B. and Borchiellini, C. (2015). *Oscarella lobularis* (Homoscleromorpha, Porifera) regeneration: epithelial morphogenesis and metaplasia. *PLoS ONE* **10**, e0134566. doi:10.1371/journal.pone.0134566
- Funayama, N. (2010). The stem cell system in demosponges: insights into the origin of somatic stem cells. *Develop. Growth Differ.* **52**, 1–14. doi:10.1111/j.1440-169X.2009.01162.x
- Gaino, E. and Burlando, B. (1990). Sponge cell motility: a model system for the study of morphogenic processes. *Bollettino di Zoologia* **57**, 109–118. doi:10.1080/11250009009355684
- Glazer, R. I., Vo, D. T. and Penalva, L. O. (2012). Musashi1: an RBP with versatile functions in normal and cancer stem cells. *Front. Biosci.* **17**, 54–64. doi:10.2741/3915
- Grotendorst, G. R., Grotendorst, C. A. and Gilman, T. (1988). Production of growth factors (PDGF & TGF- β) at the site of tissue repair. *Prog. Clin. Biol. Res.* **266**, 47–54.
- Grzelkowska, K., Zimowska, W., Skierski, J., Wareński, P., Płoszaj, T. and Trzeciak, L. (1998). Expression of bcl-2 and bax in TGF- β 1-induced apoptosis of L1210 leukemic cells. *Eur. J. Cell Biol.* **75**, 367–374. doi:10.1016/S0171-9335(98)80070-8
- Herpin, A., Lelong, C. and Favrel, P. (2004). Transforming growth factor- β -related proteins: an ancestral and widespread superfamily of cytokines in metazoans. *Dev. Comp. Immunol.* **28**, 461–485. doi:10.1016/j.dci.2003.09.007
- Hinck, A. P. (2012). Structural studies of the TGF- β s and their receptors—insights into evolution of the TGF- β superfamily. *FEBS Lett.* **586**, 1860–1870. doi:10.1016/j.febslet.2012.05.028
- Hino, K., Satou, Y., Yagi, K. and Satoh, N. (2003). A genomewide survey of developmentally relevant genes in *Ciona intestinalis*. VI. Genes for Wnt, TGF β , Hedgehog and JAK/STAT signaling pathways. *Dev. Genes Evol.* **213**, 264–272. doi:10.1007/s00427-003-0318-8
- Imhoff, J. M. and Garrone, R. (1983). Solubilization and characterization of *Chondrosia reniformis* sponge collagen. *Connect. Tissue Res.* **11**, 193–197. doi:10.3109/03008208309004855
- Inman, G. J., Nicolas, F. J., Callahan, J. F., Harling, J. D. and Gaster, L. M. (2002). SB-431542 is a potent and specific inhibitor of transforming growth factor- β superfamily type I activin receptor-like kinase (ALK) receptors ALK4, ALK5, and ALK7. *Mol. Pharmacol.* **62**, 65–74. doi:10.1124/mol.62.1.65
- Ishizuya-Oka, A., Shimizu, K., Sakakibara, S., Okano, H. and Ueda, S. (2003). Thyroid hormone-upregulated expression of Musashi-1 is specific for progenitor cells of the adult epithelium during amphibian gastrointestinal remodeling. *J. Cell Sci.* **116**, 3157–3164. doi:10.1242/jcs.00616
- James, D., Levine, A. J., Besser, D. and Hemmati-Brivanlou, A. (2005). TGF β /activin/nodal signaling is necessary for the maintenance of pluripotency in human embryonic stem cells. *Development* **132**, 1273–1282. doi:10.1242/dev.01706
- Junqueira, L. C., Bignolas, G. and Brentani, R. R. (1979). Picrosirius staining plus polarization microscopy, a specific method for collagen detection in tissue sections. *Histochem. J.* **11**, 447–455. doi:10.1007/BF01002772
- Kaartinen, V., Voncken, J. W., Shuler, C., Warburton, D., Bu, D., Heisterkamp, N. and Groffen, J. (1995). Abnormal lung development and cleft palate in mice

- lacking TGF- β 3 indicates defects of epithelial-mesenchymal interaction. *Nat. Genet.* **11**, 415-421. doi:10.1038/ng1295-415
- Kenny, N. J., De Goeij, J. M., De Bakker, D. M., Whalen, C. G., Berezikov, E. and Riesgo, A.** (2018). Towards the identification of ancestrally shared regenerative mechanisms across the Metazoa: a transcriptomic case study in the desmopage *Halisarca caerulea*. *Mar. Genomics* **37**, 135-147. doi:10.1016/j.margen.2017.11.001
- Kreuter, J., Müller, W., Swatschek, D., Schatton, W. and Schatton, M.** (2000). Method for isolating sponge collagen and producing nanoparticulate collagen, and the use thereof. US Patent 20030032601 A1, 3 March 2000.
- Letterio, J. J. and Roberts, A. B.** (1998). Regulation of immune responses by TGF β . *Annu. Rev. Immunol.* **16**, 137-161. doi:10.1146/annurev.immunol.16.1.137
- Letunic, I., Doerks, T. and Bork, P.** (2008). SMART 6: recent updates and new developments. *Nucleic Acids Res.* **37**, D229-D232. doi:10.1093/nar/gkn808
- Matsuoka, J. and Grotendorst, G. R.** (1989). Two peptides related to platelet-derived growth factor are present in human wound fluid. *Proc. Natl. Acad. Sci. USA* **86**, 4416-4420. doi:10.1073/pnas.86.12.4416
- Müller, W. E. G.** (1998). Origin of Metazoa: sponges as living fossils. *Naturwissenschaften* **85**, 11-25. doi:10.1007/s001140050444
- Nickel, M. and Brümmer, F.** (2003). In vitro sponge fragment culture of *Chondrosia reniformis* (Nardo, 1847). *J. Biotechnol.* **100**, 147-159. doi:10.1016/S0168-1656(02)00256-0
- Nicklas, M., Schatton, W., Heinemann, S., Hanke, T. and Kreuter, J.** (2009). Enteric coating derived from marine sponge collagen. *Drug Dev. Ind. Pharm.* **35**, 1384-1388. doi:10.3109/03639040902939239
- Okamoto, K., Nakatsukasa, M., Alié, A., Masuda, Y., Agata, K. and Funayama, N.** (2012). The active stem cell specific expression of sponge *Musashi* homolog *EFMsIA* suggests its involvement in maintaining the stem cell state. *Mech. Dev.* **129**, 24-37. doi:10.1016/j.mod.2012.03.001
- O'Kane, S. and Ferguson, M. W.** (1997). Transforming growth factor beta s and wound healing. *Int. J. Biochem. Cell Biol.* **29**, 63-78. doi:10.1016/S1357-2725(96)00120-3
- Pang, K., Ryan, J. F., Baxeavanis, A. D. and Martindale, M. Q.** (2011). Evolution of the TGF- β signaling pathway and its potential role in the ctenophore, *Mnemiopsis leidyi*. *PLoS One* **6**, e24152. doi:10.1371/journal.pone.0024152
- Piek, E., Heldin, C. H. and Ten Dijke, P.** (1999). Specificity, diversity, and regulation in TGF- β superfamily signaling. *FASEB J.* **13**, 2105-2124. doi:10.1096/fasebj.13.15.2105
- Pohlars, D., Brenmoehl, J., Löffler, I., Müller, C. K., Leipner, C., Schultze-Mosgau, S., Stallmach, A., Kinne, R. W. and Wolf, G.** (2009). TGF- β and fibrosis in different organs – molecular pathway imprints. *Biochim. Biophys. Acta* **1792**, 746-756. doi:10.1016/j.bbadis.2009.06.004
- Pozzolini, M., Bruzzzone, F., Berilli, V., Mussino, F., Cerrano, C., Benatti, U. and Giovine, M.** (2012). Molecular characterization of a nonfibrillar collagen from the marine sponge *Chondrosia reniformis* Nardo 1847 and positive effects of soluble silicates on its expression. *Mar. Biotechnol.* **14**, 281-293. doi:10.1007/s10126-011-9415-2
- Pozzolini, M., Mussino, F., Cerrano, C., Scarfi, S. and Giovine, M.** (2014). Sponge cell cultivation: optimization of the model *Petrosia ficiformis* (Poiret 1789). *Exp. Mar. Biol. Ecol.* **454**, 70-77. doi:10.1016/j.jembe.2014.02.004
- Pozzolini, M., Scarfi, S., Mussino, F., Ferrando, S., Gallus, L. and Giovine, M.** (2015). Molecular cloning, characterization, and expression analysis of a Prolyl 4-Hydroxylase from the marine sponge *Chondrosia reniformis*. *Mar. Biotechnol.* **17**, 393-407. doi:10.1007/s10126-015-9630-3
- Pozzolini, M., Ferrando, S., Gallus, L., Gambardella, C., Ghignone, S. and Giovine, M.** (2016a). Aquaporin in *Chondrosia reniformis* Nardo, 1847 and its possible role in the interaction between cells and engulfed siliceous particles. *Biol. Bull.* **230**, 220-232. doi:10.1086/BBLV230n3p220
- Pozzolini, M., Scarfi, S., Mussino, F., Ghignone, S., Vezzulli, L. and Giovine, M.** (2016b). Molecular characterization and expression analysis of the first Porifera tumor necrosis factor superfamily member and of its putative receptor in the marine sponge *C. reniformis*. *Dev. Comp. Immunol.* **57**, 88-98. doi:10.1016/j.dci.2015.12.011
- Pozzolini, M., Scarfi, S., Gallus, L., Ferrando, S., Cerrano, C. and Giovine, M.** (2017). Silica-induced fibrosis: an ancient response from the early metazoans. *J. Exp. Biol.* **220**, 4007-4015. doi:10.1242/jeb.166405
- Pozzolini, M., Scarfi, M., Gallus, L., Castellano, M., Vicini, S., Cortese, K., Gagliani, M. C., Bertolino, M., Costa, G. and Giovine, G.** (2018). Production, characterization and biocompatibility evaluation of collagen membranes derived from marine sponge *Chondrosia reniformis* Nardo, 1847. *Mar. Drugs* **16**, 111. doi:10.3390/md16040111
- Riesgo, A., Farrar, N., Windsor, P., Giribet, G. and Leys, S. P.** (2014). The analysis of eight transcriptomes from all Porifera classes reveals surprising genetic complexity in sponges. *Mol. Biol. Evol.* **31**, 1102-1120. doi:10.1093/molbev/msu057
- Rohmquist, F. and Huelsenbeck, J. P.** (2003). MrBayes 3: Bayesian phylogenetic inference under mixed models. *Bioinformatics* **19**, 1572-1574. doi:10.1093/bioinformatics/btg180
- Sanford, L. P., Ormsby, I., Gittenberger-de Groot, A. C., Sariola, H., Friedman, R., Boivin, G. P., Cardell, E. L. and Doetschman, T.** (1997). TGF β 2 knockout mice have multiple developmental defects that are non-overlapping with other TGF β 2 knockout phenotypes. *Development* **124**, 2659-2670.
- Saper, C. B.** (2009). A guide to the perplexed on the specificity of antibodies. *J. Histochem. Cytochem.* **57**, 1-5. doi:10.1369/jhc.2008.952770
- Saper, C. B. and Sawchenko, P. E.** (2003). Magic peptides, magic antibodies: guidelines for appropriate controls for immunohistochemistry. *J. Comp. Neurol.* **465**, 161-163. doi:10.1002/cne.10858
- Savage-Dunn, C. and Padgett, R. W.** (2017). The TGF- β family in *Caenorhabditis elegans*. *Cold Spring Harb. Perspect. Biol.* **9**, a022178. doi:10.1101/cshperspect.a022178
- Scarfi, S.** (2016). Use of bone morphogenetic proteins in mesenchymal stem cell stimulation of cartilage and bone repair. *World J. Stem. Cells* **8**, 1-12. doi:10.4252/wjsc.v8.i1.1
- Suga, H., Ono, K. and Miyata, T.** (1999). Multiple TGF- β receptor related genes in sponge and ancient gene duplications before the parazoan-eumetazoan split. *FEBS Lett.* **453**, 346-350. doi:10.1016/S0014-5793(99)00749-8
- Swatschek, D., Schatton, W., Kellermann, J., Müller, W. and Kreuter, J.** (2002). Marine sponge collagen: Isolation, characterization and effects on the skin parameters surface-pH, moisture and sebum. *Eur. J. Pharm. Biopharm.* **53**, 107-113. doi:10.1016/S0939-6411(01)00192-8
- Tanaka, E. M. and Reddien, P. W.** (2011). The cellular basis for animal regeneration. *Dev. Cell* **21**, 172-185. doi:10.1016/j.devcel.2011.06.016
- Tanaka, K. and Watanabe, Y.** (1984). Choanocyte differentiation and morphogenesis of choanocyte chambers in the fresh-water sponge, *Ephydatia fluviatilis*, after reversal of developmental arrest caused by hydroxyurea. *Zool. Sci.* **1**, 561-540.
- Upadhyay, A., Moss-Taylor, L., Kim, M. J., Ghosh, A. C. and O'Connor, M. B.** (2017). TGF- β family signaling in *Drosophila*. *Cold Spring Harb. Perspect. Biol.* **9**, a022152. doi:10.1101/cshperspect.a022152
- Vandesompele, J., De Preter, K., Pattyn, F., Poppe, B., Van Roy, N., De Paepe, A. and Speleman, F.** (2002). Accurate normalization of real-time quantitative RT-PCR data by geometric averaging of multiple internal control genes. *Genome Biol.* **3**, RESEARCH0034. doi:10.1186/gb-2002-3-7-research0034
- Van Soest, R. W. M., Boury-Esnault, N., Vacelet, J., Dohrmann, M., Erpenbeck, D., De Voogd, N. J., Santodomingo, N., Vanhoorne, B., Kelly, M. and Hooper, R. W. M.** (2012). Global diversity of sponges (Porifera). *PLoS ONE* **7**, e35105. doi:10.1371/journal.pone.0035105
- Van Wolfswinkel, J. C.** (2014). Piwi and potency: PIWI proteins in animal stem cells and regeneration. *Integr. Comp. Biol.* **54**, 700-713. doi:10.1093/icb/ucu084
- Vervoort, M.** (2011). Regeneration and development in animals. *Biological Theory* **6**, 25-35. doi:10.1007/s13752-011-0005-3
- Waterhouse, A. M., Procter, J. B., Martin, D. M. A., Clamp, M. and Barton, G. J.** (2009). Jalview Version 2 – a multiple sequence alignment editor and analysis workbench. *Bioinformatics* doi:10.1093/bioinformatics/btp033
- Worheide, G., Dohrmann, M., Erpenbeck, D., Larroux, C., Maldonado, M., Voigt, O., Borchiellini, C. and Lavrov, D. V.** (2012). Deep phylogeny and evolution of sponges (Phylum Porifera). *Adv. Mar. Biol.* **61**, 1-78. doi:10.1016/B978-0-12-387787-1.00007-6
- Zhang, W., Zhang, X., Cao, X., Xu, J., Zhao, Q., Yu, X., Jin, M. and Deng, M.** (2003). Optimizing the formation of in vitro sponge primmorphs from the Chinese sponge *Stylotella agminate* (Ridley). *J. Biotechnol.* **100**, 161-168. doi:10.1016/S0168-1656(02)00255-9